ANALYSIS OF TRANSVERSE IMPACT ON BEAMS

BY
VIJAY KUMAR JADON

DEPARTMENT OF MECHANICAL ENGINEERING
INDIAN INSTITUTE OF TECHNOLOGY KANPUR
AUGUST 1971

ANALYSIS OF TRANSVERSE IMPACT ON BEAMS

A Thesis Submitted
In Partial Fulfilment of the Requirements
for the Degree of
MASTER OF TECHNOLOGY

BY
VIJAY KUMAR JADON

to the

DEPARTMENT OF MECHANICAL ENGINEERING
INDIAN INSTITUTE OF TECHNOLOGY KANPUR
AUGUST 1971

TO

MY PARENTS

CERTIFICATE

This is to certify that the thesis entitled 'Analysis of Transverse Impact on Beams' by V.K. Jadon is a record of work carried out under my supervision and has not been submitted elsewhere for a degree.

V.Sundararajan
Assistant Professor
Department of Mechanical Engg.
Indian Institute of Technology
Kanpur

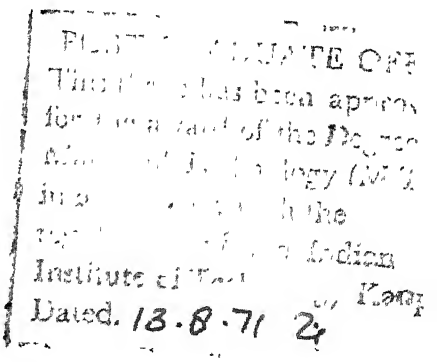

ACKNOWLEDGEMENTS

I would like to express my deep appreciation and gratitude to

Dr. V. Sundararajan and Dr. L.S. Srinath to whom I am indebted for their continuous guidance and unending encouragement which were vital to the success of this effort,

The National Bureau of Standards (U.S. Department of Commerce) for supporting this project.

Thanks are also due to

Dr. A.B.L. Agarwal who found time for me for many interesting and fruitful discussions for the instrumentation involved in the experiments,

Mr.M.M. Singh for his continuous help in conducting the experiments,

Mr. Uma Raman Pandey for his excellent and efficient typing,

All my friends for their constructive criticisms, help and friendship.

VIJAY KUMAR JADON

CONTENTS

PAGE

LIST OF TABLES

LIST OF FIGURES

PAGE

LIST OF PLATES

NOMENCLATURE

SYMBOLS	MEANING
$W(x,t)$	Beam Deflection
ϵ	Strain
F	Impact Force
w	Striker Displacement
K	Hertz Constant
V_o	Striking Velocity of Striker
ρ	Mass Density of Beam material
d	Depth of beam
h	Height of beam
M_1	Mass of beam
m_2	Mass of Striker
M	Mass ratio = M_1/M_2
L	Length of beam
A	Cross section of beam = d·h
ν	Poisson's ratio
i	Show the states of vibration of beam
ω_i	Eigen frequency $= \frac{i^2\pi^2}{L^2}\left(\frac{EI}{d\rho h}\right)^{1/2}$
C_i	Eigen function $= \text{Sin}\ \frac{i\pi x}{L}$ for simply supported beam

α Beam parameter $= \sqrt{\frac{2}{\pi}} \cdot \frac{1}{d\rho h} \cdot \left(\frac{d\rho h}{EI}\right)^{1/4}$

T Reference time $= \frac{M_2^{2/5}}{K^{2/5} V_o^{1/5}}$.

τ Dimensionless time variable $= \frac{t}{T}$.

λ Impact parameter $= \frac{\alpha M_2}{T^{1/2}}$

f Dimensionless strain

$\sigma^{3/2}$ Dimensionless force.

SYNOPSIS

of the
Dissertion on

ANALYSIS OF TRANSVERSE IMPACT ON BEAMS

Submitted in Partial Fulfilment of
the Requirements for the Degree

of

MASTER OF TECHNOLOGY

in

MECHANICAL ENGINEERING

by
VIJAY KUMAR JADON
Department of Mechanical Engineering
Indian Institute of Technology, Kanpur

Analysis of transverse impact behaviour of simply supported and built-in beam is investigated in the present work, with and without taking into account the contact deformation. The impact is assumed to be purely elastic. Hertz's law for contact deformation is assumed to hold.

Experiments have been conducted to verify the theoretical prediction. Non-dimensional impact force, and maximum strain have to be plotted against impact parameter which depends on geometries and the elastic properties of the beam and striker.

CHAPTER 1

INTRODUCTION

1.1 TRANSVERSE IMPACT ON BEAM

During the last four decades, scientists and engineers have exhibited an increasing interest in the solution of problems concerned with the dynamic loading on structures, particularly in the case of impact. Actual examples of this type of loading may be found in the fields of tool design, foundry and machine shop operations, protective ordnance, vehicle accidents and in many other areas.

But the severe mathematical complexity encountered in treating the problem as a whole restricts the study of impact phenomena to impact involving only simple type of geometry; and in the case of machine or building structures the simplest and most important type of structural element would be a simply-supported or built-in beam subjected to a transverse impact load.

The duration of impact, the maximum impact force exerted and peak values of stress or deflection are the quantities of interest for such a situation. In the neighbourhood of impact point the transient stress distribution is obviously three dimensional; the waves are not only propagated along the beam but

are also reflected from all surfaces. At more distant stations the stress will be more uniformly distributed across the width, exhibiting the well known bending features with stress variation at a given cross section occuring primarily as a function of depth. This pattern also extends to the region of contact point after removal of load. Because of analytical and experimental limitations the three dimensional theory does not appear to be feasible.

In order to make the problem amenable to theoretical treatment it is assumed that the variation of stress across the width can be neglected. Thus the problem boils down to a two dimensional problem of plane stress. Additional simplification is brought in by neglecting the rotary inertia and transverse shear.

1.2 HISTORICAL DEVELOPMENT

In the field of one dimensional transverse impact on beams many scientific research workers have contributed various analytical and experimental approaches. Various mathematical models to the problem have been suggested since 1800 for the solution. The simple approximation for elastic deflection of a beam under transverse horizontal impact obtained by equating the energy of striking body to the resilience of beam may be attributed to Young[1]. Hodgkinson [2]analysed the

problem with simple consideration of momentum transfer and justified them with experiments. His results were given a theoretical basis by an important analytical investigation made by Cox [3] to explain the results of a Royal Commission's experiments [4]. Later a complete solution was presented by Saint Venant and A.Flament [5] who recognised the presence of vibratory motion which materially influenced the form of elastic curve. The nineteenth century investigators attempted to rationalise experimental results with vibration theories by postulating the existence of a quasi-elastic layer near the contact point. This concept was superceeded by the theory of local contact deformations introduced by Hertz [6] which has found wide use in spite of the static elastic nature of its derivation.

Realizing that the local deformation of the contact region was an important influence, Timeshenko [7] devised a solution combining the contact pressure equation of Hertz with the lateral vibration theory. Solving the differential equation of forced vibration under a central force varying arbitrarily with time, he related the beam deflection and local deformation to the striking mass displacement. His extensive work paved the way for further investigations with more modifications in the mathematical models and verifications by the experiments.

Zener [8] calculated the energy losses during impact and gave an experimental verification. A further simplification in the analysis for the impact problem was done by E.H. Lee [9] in his Doctoral Thesis. He assumed that because the duration of impact is small compared to the fundamental time period of the beam, first mode of vibration of the beam is sufficient to be considered for the analysis. But in some cases, particularly for impacts with large energies, the results obtained did not confirm the earlier theory given by Timoshenko. Mason [10] showed in his experiments the influence of multiple collisions by the striker, particularly when the striker mass or the striking velocity is increased. In the field of photostress analysis extensive work was done by Föppl [11] to verify the result with Timoshenko's Theory. Galerkin's technique and Collocation method have been used by Eringen [12] in deriving approximate and quickly solvable results.

During the last decade experiments were conducted by Horst Schwieger [13, 14] with steel spheres impacting on beams. He assumed that because the impact duration is much less than the natural time period of the beam, in the vicinity of contact point the peaks of stress and force occur much earlier than the arrival of the reflected waves and so they are unaffected by the boundary conditions.

1.3 PRESENT WORK

In the present investigation two different independent mathematical methods have been suggested for the analysis of the impact problem. The first one does not consider the contact deformations while the second one takes into account the relative approach of the bodies during the process of contact.

Experiments have been performed to verify the theoretical predictions. Effects of impact velocities, the mass of the striker, boundary conditions etc. have been studied for various beams. Applicability of both the mathematical methods has been studied comparing the results predicted by them with the experimental values. Non-dimensional quantities such as maximum impact force, maximum stress have been plotted against a non-dimensional parameter (λ) in order to predict quickly the maximum stress developed in a structural element subjected to an impact with a known mass and striker velocity. Influence of various parameters of beams and the striker (such as the striker velocity and geometry) on the value of impact parameter λ has been studied.

CHAPTER 2

ANALYTICAL INVESTIGATION

2.1 MATHEMATICAL MODELS

In the analytical investigation two models are considered. In the first the effect of the contact deformations of the structural element due to the striker mass is neglected. This implies that the displacement of the striker and the beam at the impact point are assumed to be the same (fig.1, model 1), that is,

$$W_o\left(\frac{L}{2}, t\right) = w(t) \qquad (2.1.1)$$

where W_o = Displacement of beam at impact point

w = Displacement of striker mass

$\frac{L}{2}$ = C = striking point on the beam.

In the second model the effect of local contact deformations of the beam due to the striker is taken into account, that is, there is a relative motion between the striker and the beam during the impact. This relative motion (fig.1, model 2), $w - W_o$ is given by the Hertz's contact deformation equation as follows for purely elastic impact.

$$F(t) = K\left[w(t) - W_o\left(\frac{L}{2}, t\right)\right]^{3/2} \qquad (2.1.2)$$

where K, the Hertz constant, depends upon the material properties of the two bodies and their geometries. For

the case of cylindrical shaped striker with hemispherical end and the beam, it would be [15]

$$K = \frac{2}{3} \frac{E}{1-\nu^2} r^2 \qquad (2.1.3)$$

where $E_1 = E_2 = E$ = Modulus of elasticity for beam and striker material;

$\nu_1 = \nu_2 = \nu$ = Poisson's ratio for both the beam and the hammer and

r = radius of the hemispherical end of the hammer.

The following assumptions have been made in both the mathematical models :

(a) Natural frequency of free vibrations of the striker is very high. Therefore its any type of effect is neglected.

(b) Collision is perfectly elastic that is no permanent indentations occur in the two colliding bodies at the point of contact.

(c) The supports are ideal. They do not absorb any part of energy during the impact.

(d) Presence of only one collision during the impact is assumed. For higher initial velocities, multiple collisions take place and they affect the occurrance of peak values of impact force or strain (fig. 2).

2.2 ANALYSIS WITH NO CONTACT DEFORMATION

An approximate method is developed here wherein the beam vibration equation is solved and the applied impulse is replaced by a suitable initial condition [5, 15]. The equation of motion for the transverse vibration of a beam is

$$E I \frac{\partial^4 W}{\partial x^4} + \rho A \frac{\partial^2 W}{\partial t^2} = 0 \qquad (2.2.1)$$

where E = Young's modulus of elasticity for beam

I = Moment of inertia of the beam cross section

ρ = Mass density

A = Cross section of the beam.

The solution of the above equation can be written as

$$W(x,t) = \sum_{i=1}^{\infty} \left[A_i \sin \xi_i x + B_i \cos \xi_i x + C_i \sin h \xi_i x + D_i \cos h \xi_i x \right] \cdot \left[E_i \sin \omega_i t + F_i \cos \omega_i t \right] \qquad (2.2.2)$$

where

$\xi_i^2 a^2 = \omega_i$ = Eigen frequency, and

$$a^4 = \frac{EI}{\rho A}$$

Substituting the following boundary conditions for simply supported end conditions in eq.(2.2.2),

$$W(0,t) = 0 \tag{2.2.3}$$

$$\frac{\partial^2 W}{\partial x^2}(0,t) = 0 \tag{2.2.4}$$

$$\frac{\partial W}{\partial x}\left(\frac{L}{2},t\right) = 0 \tag{2.2.5}$$

The constants $B_i = D_i = 0$ and,

$$C_i = -A_i \mathrm{Cos}\left(\frac{\xi_i L}{2}\right)/\mathrm{Cos\ h}\left(\frac{\xi_i L}{2}\right)$$

With the initial condition

$$W(x,0)=0 \tag{2.2.6}$$

the value of $F_i = 0$. And finally the eq.(2.2.2) reduces to the following form

$$W(x,t)= \sum_{i=1}^{\infty} \frac{1}{a^2 \xi_i^2} G_i X_i \mathrm{Sin}(\xi_i^2 a^2 t) \tag{2.2.7}$$

where, $G_i = a^2 \xi_i^2 E_i A_i \mathrm{Cos}(\frac{1}{2} \xi_i L)$ (2.2.8)

and,

$$X_i=\mathrm{Sin}(\xi_i x)/\mathrm{Cos}\left(\frac{\xi_i L}{2}\right) - \mathrm{Sinh}(\xi_i x)/\mathrm{Cosh}\left(\frac{\xi_i L}{2}\right) \tag{2.2.9}$$

Substitution of eq.(2.2.7) in the following boundary condition

$$EI \frac{\partial^3 W}{\partial x^3}\left(\frac{L}{2}, t\right)= \frac{1}{2} m_2 \frac{\partial^2 W}{\partial t^2}\left(\frac{L}{2}, t\right) \tag{2.2.10}$$

yields the characteristic equation in ϕ_i as follows,

$$\phi_i(\tan \phi_i - \tanh \phi_i) = 2M \qquad (2.2.11)$$

where M = Mass ratio = M_1/m_2 (2.2.12)

$$\phi_i = \frac{\xi_{ji} L}{2}, \qquad i = 1,2,\ldots\ldots \infty \qquad (2.2.13)$$

Evaluation of G_i of the eq.(2.2.7) involves replacement of the impulsive force by an initial velocity condition for the beam. It will be assumed here that the striker imparts a velocity indistinguishable from V_o to an infinitesimal section of the beam just at the point of contact. Then, momentum of this section and striker should be equal to the initial momentum $m_2 V_o$ that is,

$$\int \frac{\partial W}{\partial t}(x,0)\, d\bar{Q} = m_2 V_o \qquad (2.2.14)$$

where integration is carried out with respect to the total mass of the beam and striker.

From eq.(2.2.7),

$$\frac{\partial W}{\partial t}(x,0) = \sum_{i=1}^{\infty} G_i X_i = \psi(x) \qquad (2.2.15)$$

or,

$$\sum_{i=1}^{\infty} G_i X_i X_j = \psi(x) X_j \qquad (2.2.16)$$

$$j = 1,2,\ldots\ldots \infty$$

If eq.(2.2.16) is multiplied by m_2 and evaluated at $x = \frac{L}{2}$ and added to the integral of eq.(2.2.16) with respect to beam mass $dm_1 = m_1/L\ dx$, there is obtained in view of symmetry,

$$\sum_{i=1}^{\infty} G_i \left\{ \frac{2m_1}{L} \int_0^{L/2} X_i X_j\, dx + m_2 X_i\left(\frac{L}{2}\right) X_j\left(\frac{L}{2}\right) \right\}$$

$$= \frac{2m_1}{L} \int_0^{L/2} X_j \psi(x)\, dx + m_2 X_j\left(\frac{L}{2}\right) \psi\left(\frac{L}{2}\right) \qquad (2.2.17)$$

which is just the representation of integral in eq.(2.2.14). Utilising the orthogonality of X_i and X_j,

$$G_i = \frac{\frac{2m_1}{L} \int_0^{L/2} X_i \psi(x)dx + m_2 X_i\left(\frac{L}{2}\right) \psi(L/2)}{\frac{2m_1}{L} \int_0^{L/2} X_i^2\, dx + m_2 X_i^2\,(L/2)} \qquad (2.2.18)$$

Applying the initial conditions at $t = 0$,

$$\frac{\partial W}{\partial t} = 0 = \psi(x) \quad \text{for} \quad x \neq \frac{L}{2} \qquad (2.2.19)$$

$$\frac{\partial W}{\partial t} = V_o = \psi(L/2) \text{ for } x = \frac{L}{2} \qquad (2.2.20)$$

eq.(2.2.18) is reduced to the following form :

$$G_i = \frac{m_2 V_o X_i (L/2)}{\frac{2m_1}{L}\int_0^{L/2} X_i^2 dx + m_2 X_i^2 (L/2)}$$

$$= \frac{4V_o}{\phi_i\left[\frac{1}{\cos^2\phi_i} - \frac{1}{\cosh^2\phi_i}\right] + \frac{2M}{\phi_i}} \qquad (2.2.21)$$

Finally substitution of eq.(2.2.21) in eq.(2.2.7) gives for simply supported end conditions,

$$W(x,t) = \frac{L^2 V_o}{a^2} \sum_{i=1}^{\infty} \frac{1}{\phi_i^3} \cdot \frac{\sin\frac{2\phi_i x}{L}}{\cos\phi_i} - \frac{\sinh\frac{2\phi_i x}{L}}{\cosh\phi_i} \Big/ \frac{1}{\cos^2\phi_i} - \frac{1}{\cosh^2\phi_i} + \frac{2M}{\phi_i^2} \cdot \sin\frac{4\phi_i^2 a^2}{L^2} t \qquad (2.2.22)$$

Similarly for clamped end conditions the expression for deflection is

$$W(x,t) = \frac{V_o L^2}{2a^2} \sum_{i=1}^{\infty} \frac{1}{\phi_i^2} \cdot \left[\frac{(1-\cos\phi_i\cosh\phi_i)(\cos\phi_i-\cosh\phi_i)(\sin\phi_i+\sinh\phi_i)}{(1-\cos\phi_i\cosh\phi_i)^2 + M(\cos\phi_i-\cosh\phi_i)^2}\right] \cdot \left[\frac{\sinh\frac{2\phi_i x}{L} - \sin\frac{2\phi_i x}{L}}{\cosh\phi_i - \cos\phi_i} - \frac{\cosh\frac{2\phi_i x}{L} - \cos\frac{2\phi_i x}{L}}{\sinh\phi_i + \sin\phi_i}\right] \sin\left(\frac{4\phi_i^2 a^2 t}{L^2}\right) \qquad (2.2.23)$$

where $\emptyset_i$'s are determined from the following characteristic equation,

$$M = \frac{\emptyset_i(1-\text{Cos}\emptyset_i\text{Cosh}\,\emptyset_i)}{\text{Sin}\,\emptyset_i\text{Cosh}\emptyset_i+\text{Cos}\emptyset_i\text{Sinh}\emptyset_i} \qquad (2.2.24)$$

Strain is obtained by differentiating eqs.(2.2.22) and (2.2.23) twice with respect to x and then substituting it in following equation

$$\epsilon(x,t) = \frac{H}{2}\,\frac{\partial^2 w}{\partial x^2} \qquad (2.2.25)$$

The impact force F(t) is evaluated by knowing acceleration from eqn.(2.2.22) and (2.2.23) and then multiplying it by mass of striker m_2 as follows

$$F(t) = m_2\,\frac{\partial^2 w}{\partial t^2}\left(\frac{L}{2},\, t\right) \qquad (2.2.26)$$

Numerical methods and results are discussed in Chapter 4. Unfortunately convergence in the case of eqs.(2.2.25) and (2.2.26) is very poor and results have been provided with consideration of first ten harmonics.

2.3 ANALYSIS WITH CONTACT DEFORMATION

In this section the local contact deformations of the beam and the striker are taken into account. The response of the beam and the impact force are calculated using

i) the Hertz's Law [eq.(2.1.2)]

ii) the Dynamics of Hammer

From the available standard methods [15, 13] for the solution of beam subjected to a force varying arbitrarily with time and acting at distance x = C, the deflection of beam is given as follows :

$$W(x,t) = \sum_{i=1}^{\infty} X_i \left[q_o \cos(\omega_i t) + \frac{\dot{q}_o}{\omega_i} \sin(\omega_i t) \right.$$

$$\left. + \frac{X_i(C)}{\rho A \omega_i \int_0^L X_i^2 dx} \cdot \int_0^t F(\tau') \cdot \sin \omega_i (t - \tau') d\tau' \right] \qquad (2.3.1)$$

where

ω_i = Eigen frequency of beam (2.3.2)

X_i = Eigen function of beam (2.3.3)

ρ = Mass density of beam material (2.3.4)

A = Uniform cross-section of beam (2.3.5)

$q_o \sum_{i=1}^{\infty} X_i$ = Initial displacement of beam (2.3.6)

$\dot{q}_o \sum_{i=1}^{\infty} X_i/\omega_i$ = Initial velocity of beam (2.3.7)

For the beam initially at rest, expressions (2.3.6) and (2.3.7) become zero, and eq.(2.3.1) reduces to

$$W(x,t) = \frac{1}{\rho A} \sum_{i=1}^{\infty} \frac{X_i^2(C)}{\omega_i \int_0^L X_i^2 dx} \left[\int_0^t F(\tau') \operatorname{Sin} \omega_i (t-\tau') d\tau' \right] \qquad (2.3.8)$$

For a simply supported beam,

$$\omega_i = \frac{i^2 \pi^2}{L^2} \left(\frac{EI}{d \rho h} \right)^{1/2} \qquad (2.3.9)$$

$$X_i = \operatorname{Sin} (i\pi x/L) \qquad (2.3.10)$$

$$\int_0^L X_i^2 dx = L/2 \qquad (2.3.11)$$

and force acting at $x = C = L/2$, the eq.(2.3.6) yields,

$$W(\frac{L}{2},t) = W_o(\frac{L}{2},t) = \frac{1}{\rho A} \sum_{i=1}^{\infty} \frac{\operatorname{Sin}^2(\frac{i\pi}{2})}{\omega_i . L/2} \cdot \left[\int_0^t F(\tau') \operatorname{Sin} \omega_i (t-\tau') d\tau' \right] \qquad (2.3.12)$$

Rearranging the above equation following one is obtained :

$$W_o(\frac{L}{2},t) = \frac{2}{\rho AL} \int_0^t F(\tau') \cdot \left[\sum_{i=1}^{\infty} \frac{\operatorname{Sin}^2(i\pi/2)}{\omega_i} \operatorname{Sin} \omega_i (t-\tau') \right] d \qquad (2.3.13)$$

The value of $\operatorname{Sin}^2(i\pi/2)$ fluctuates between the limits +1 and -1. Thus representation of summation sign in eq.(2.3.13) in the form of integration is

possible [16] or,

$$\sum_{i=1}^{\infty} \frac{\mathrm{Sin}^2(i\pi/2)}{\omega_i} \mathrm{Sin}\,\omega_i(t-\tau') = \tfrac{1}{2}\int_0^{\infty} \frac{\mathrm{Sin}\ (t-\tau')}{\omega}\, di \qquad (2.3.14)$$

where i means continuously varying quantity of the states of vibration and is given by

$$i = L/(\bar{\lambda}/2) = \omega L/(\pi . C_v) \qquad (2.3.15)$$

where

C_v = phase velocity

$\omega = \omega(i)$

From eqs.(2.3.15) and (2.3.9)

$$di = i\,\frac{d\omega}{\omega} = \frac{\omega}{\pi/L} \cdot \left(\frac{d\rho h}{EI}\right)^{1/4} \cdot \frac{d\omega}{\omega} = \frac{L}{\pi} \cdot \left(\frac{d\rho h}{EI}\right)^{1/4} \cdot \omega^{-1/2} d \qquad (2.3.16)$$

The integral in eq.(2.3.14) becomes

$$\int_0^{\infty} \frac{\mathrm{Sin}\ \omega(t-\tau')}{\omega} \cdot \frac{L}{\pi} \cdot \left(\frac{d\rho h}{EI}\right)^{1/4} \cdot \omega^{-1/2}\, d\omega$$

$$= \frac{L}{\pi} \cdot \left(\frac{d\rho h}{EI}\right)^{1/4} \cdot \sqrt{2\pi} \cdot (t-\tau')^{1/2} \qquad (2.3.17)$$

Substitution of eq.(2.3.17) in (2.3.13) gives

$$W_o\left(\frac{L}{2},t\right) = \frac{2}{\rho AL}\int_0^t F(\tau') \cdot \tfrac{1}{2} \cdot \frac{L}{\pi} \cdot \left(\frac{d\rho h}{EI}\right)^{1/4} \cdot \sqrt{2\pi} \cdot (t-\tau')^{1/2}\, d\tau'$$

$$= \sqrt{\frac{2}{\pi}} \cdot \frac{1}{d\rho h} \cdot \left(\frac{d\rho h}{EI}\right)^{\frac{1}{4}} \cdot \int_0^t F(\tau') \cdot (t-\tau')^{1/2}\, d\tau' \qquad (2.3.18)$$

Defining a beam parameter α,

$$\alpha = \sqrt{\frac{2}{\pi}} \cdot \frac{1}{d\rho h} \cdot \left(\frac{d\rho h}{EI}\right)^{1/4} \qquad (2.3.19)$$

eq.(2.3.18) becomes

$$W_o\left(\frac{L}{2},t\right) = \alpha \int_o^t F(\tau').(t-\tau')^{1/2}\, d\tau' \qquad (2.3.20)$$

From the dynamics of hammer,

$$m_2 \frac{d^2w}{dt^2} = - F(t) \qquad (2.3.21)$$

with the following initial conditions :

$$w\Big|_{t=o} = 0 \qquad (2.3.22)$$

$$\frac{dw}{dt}\Big|_{t=o} = V_o \qquad (2.3.23)$$

Integrating twice the eq.(2.3.21) following equation is obtained for the displacement of hammer

$$w(t) = V_o\, t - \int_o^t F(\tau').(t-\tau')d\tau' \qquad (2.3.24)$$

The two eqs.(2.3.20) and (2.3.24) are related by eq.(2.1.2) as

$$F(t) = K\left[w(t) - W_o\left(\frac{L}{2},t\right)\right]^{3/2} \qquad (2.3.25)$$

where K = Hertz constant defined in eq.(2.1.3).

Substituting eqs.(2.3.20) and (2.3.24) in eq.(2.3.25)

$$K^{-2/3} F^{2/3} = V_o t - \int_o^t F(\tau').(t-\tau') \cdot \left[\frac{1}{m_2} + \alpha(t-\tau')^{-1/2} \right] d\tau' \qquad (2.3.26)$$

Defining

$$T = \frac{m_2^{2/5}}{K^{2/5} . V_o^{1/5}} = \text{Reference Time} \qquad (2.3.27)$$

and

$$\lambda' = \frac{\alpha . m_2}{T^{1/2}} = \text{Impact parameter} \qquad (2.3.28)$$

and using the dimensionless variables

$$\tau = \frac{t}{T} \qquad (2.3.29)$$

$$\sigma = \left[w(t) - W(\tfrac{L}{2}, t) \right] / T V_o \qquad (2.3.30)$$

following integral equation is obtained.

$$\sigma = \tau - \int_o^\tau \sigma^{3/2} . (\tau - \bar{\tau}) \, d\bar{\tau} - \lambda \int_o^\tau \sigma^{3/2} (\tau - \bar{\tau})^{1/2} \, d\bar{\tau} \qquad (2.3.31)$$

Proceeding on similar lines equation can be obtained for curvature at x = L/2 as follows :

$$\frac{\partial^2 W}{\partial x^2} = - \frac{L}{M_1} \frac{1}{\sqrt{2\pi}} \left(\frac{d \rho h}{EI} \right)^{3/4} \int_o^t F(\tau')(t-\tau')^{-1/2} d\tau' \qquad (2.3.32)$$

and final expression for strain will be

$$\epsilon\left(\frac{L}{2},t\right)=\sqrt{3}\left(\frac{\rho}{E}\right)^{1/2}\cdot\frac{\alpha}{2}\cdot K\cdot V_o^{3/2}\cdot T^2\cdot\int_o^{\tau}\sigma^{3/2}\cdot(\tau-\bar{\tau})^{-1/2}d\bar{\tau} \qquad (2.3.33)$$

The quality in the integral sign in eq.(2.3.33) is denoted by $f(\tau,\lambda)$ i.e.

$$f(\tau,\lambda)=\int_o^{\tau}\sigma^{3/2}(\tau-\bar{\tau})^{-1/2}\,d\bar{\tau} \qquad (2.3.34)$$

Equation (2.3.31) is solved numerically by finite Difference Method [17]; knowing σ, Impact force is calculated from eqs.(2.3.30) and (2.3.25) as follows:

$$F = K(T\,V_o)^{3/2}\cdot\sigma^{3/2} \qquad (2.3.35)$$

Deflection $W_o(\frac{L}{2},t)$ and strain $\epsilon(\frac{L}{2},t)$ are obtained respectively from eqs.(2.3.24) and (2.3.33) and (2.3.34) by the numerical procedure of integration after knowing σ or F.

CHAPTER 3

EXPERIMENTAL ARRANGEMENT

3.1 BRIEF DESCRIPTION OF THE SET UP

An experiment has been designed to verify the theoretical predictions. The experimental arrangement is given in Figure (3). Details of the set up are shown in plates 1 to 4. Beams of uniform rectangular cross sections have been tested. Table 1 gives the list of tests conducted with various hammers and beam cross sections. End supports are shown in Figures (4,5); they have been so designed that the loss of energy during the impact is minimum. This is accomplished by avoiding any sort of deformations at the support. To achieve this hard steel spheres and hardened steel flats have been used in the supports.

The hammer is supported by means of low stiffness stainless steel tube to minimise the energy absorption and also to ensure the movement of the striking mass in a vertical plane. At the top, the suspension block [fig.(6)] has been precisely made to avoid frictional forces. Sliding arrangement at the top makes possible the adjustment of the suspension point of the hammer wherever desired. Scale attached to the top supporting block measures (of the order 0.5°) the angle of swing

for the hammer. Neglecting the friction losses and assuming pendulum to be a simple one, expression for striking velocity V_o is obtained by equating the maximum potential and kinetic energies of the hammer :

$$V_o = \left[2gR\ (1 - \cos\theta)\right]^{1/2} \qquad (3.1.1)$$

where R = Length of Pendulum.

3.2 INSTRUMENTATION

In studying experimentally the response of the beam subjected to transverse impact, various parameters such as bending strain, deflection of the beam and the acceleration of the hammer during the impact have been measured. Fig.(7) shows the line diagram for the permanent record of outputs in the storage oscilloscopes and their simultaneous triggering with the acceleration signal. The very short duration of the impact (of the order 100 micro seconds) needs effective design of the electronic circuitry as well as the proper selection of the transducers for measuring various parameters involved. In the following sections transducers together with their electronics have been discussed.

3.3 ACCELERATION MEASUREMENT

For shock measurements following two types of accelerometers have been used because of their linear behaviour for a large range of acceleration and other

reasons discussed later. For detailed specification see Appendix.

1. Endevco accelerometer, Model 2215
   Working range 0 to 2000 g
   Voltage sensitivity = 14.55 pk mV/pkg
2. Endevco accelerometer, Model 2225
   Working range 100 g to 20,000 g
   Voltage sensitivity .50 pk mV/pkg.

These accelerometers using piezoelectric crystals have fairly high natural frequency of vibration (of the order 20,000 cps) and therefore they are suitable for very high response. The circuitry involved is shown in Figure (8).

Following is the formula used for calculating the voltage sensitivity of the accelerometer [18] :

$$E = E_{cal} \frac{C_p + C_{std}}{C_p + C_{cable} + C_{amp}} \qquad (3.3.1)$$

where,

E_{cal} = Voltage sensitivity of the accelerometer with standard capacitance C_{std}

C_p = Accelerometer capacitance

C_{cable} = Cable capacitance

C_{amp} = Amplifier capacitance including the residual capacitance.

3.4 STRAIN MEASUREMENT

It is obvious that the maximum bending strain occurs at the middle point of the beam when the load acts at that point. Therefore as shown in Figure (3) two gages A and B have been mounted on the back side of the beam at the middle point. They are connected to the wheatstone bridge as shown in Figure (9). Calibration of gages is done by shunting fixed resistances across the active gage [18]. The equivalent strain is given by

$$\epsilon_{equivalent} = \frac{R_g}{F_g\,(R_g + R_c)} \cdot \frac{1}{2} \qquad (3.4.1)$$

where

R_g = Gage Resistance = $120.6 \pm .2$ Ω

F_g = Gage factor = $2.06 \pm .02$

R_c = Calibration resistance

For three different calibration resistances following are the equivalent strains using eq.(3.4.1)

$\epsilon_1 \Big|_{R_c = 10^6\,\Omega}$ = 28 micro strain

$\epsilon_2 \Big|_{R_c = .51 \times 10^6\,\Omega}$ = 56 micro strain

$\epsilon_3 \Big|_{R_c = .2 \times 10^6\,\Omega}$ = 143micro strain

These values are plotted against the corresponding voltage output of the circuit in Fig. 1. And the strain sensitivity is found to be

E_b = 116.80 pk micro strain/pk mV

Temperature compensation is provided using the dummy gages in the other two arms of the bridge.

3.5 DEFLECTION MEASUREMENT

The maximum deflection will occur at the middle point of the beam for the case under consideration. So it is of main interest to measure this value. Solar cell, which utilizes a beam of light to measure the displacement is used because it has

(a) very high response because of the absence of any kind of mechanical inertia effects.

(b) high resolution without any noise in the output signal on the oscilloscope screen.

(c) linear behaviour of the solar cell for a fairly good range of displacement.

The circuit used for the solar cell is shown in Figure (10). The calibration is shown in Figure (12) and the sensitivity of the transducer is found to be

E_s = 0.00042 in/mV

For specifications of the transducer see the Appendix.

CHAPTER 4

RESULTS AND DISCUSSIONS

4.1 THEORETICAL RESULTS

The deflection of the beam at $x = \frac{L}{2}$ was obtained from eqs.(2.2.22) and (2.2.23) using IBM 7044 digital computer. The convergence of the series was very good and the first ten harmonics were sufficient. These results have been plotted in Figures (15, 19, 23, 27, 31) for all cases and it is obvious that maximum deflection obtained for clamped case is always smaller than that for simply supported case. But unfortunately the high sensitivity of second derivatives with respect to x or t of eqs. (2.2.22) and (2.2.23) makes it necessary to include more harmonics in the calculation. Particularly in case of beam with clamped ends, convergence in case of force or strain calculation is very poor [12, 19]. Inclusion of higher harmonics involves greater computational efforts in handling very large quantities (of the order e^{120}). Therefore forces and strains were calculated only for simply supported beam taking into account only the first ten harmonics.

For the second analytical approach (Sec.2.3) finite difference technique was used to solve for the non-dimensional impact force ($\sigma^{3/2}$) and non-dimensional strain (f) from eqs. (2.3.31), (2.3.34). Knowing σ and f,

other quantities like $W_o\ (\frac{L}{2}, t)$, $\epsilon\ (\frac{L}{2}, t)$, F(t) and duration of impact can be obtained. Results for all cases (see Table 1) have been shown in tables 2 to 6. In Figures (13 to 36) all the theoretical results (force, strain, displacement, time duration) together with experimental results have been plotted against V_o, or time.

4.2 EXPERIMENTAL RESULTS

For the five cases mentioned in Table 1, acceleration of hammer or the impact force ($=m_2$ x acceleration) were recorded for different striking velocities. The results have been given in Figures (13 to 36) and tables (2 to 6).

The value of E for each beam has been calculated knowing the natural frequency of fundamental mode of vibration for simply supported end conditions of the beam :

$$\omega_1 = \frac{\pi^2}{L^2}\left[EI/d\,h\right]^{1/2} \qquad (4.2.1)$$

Table 1 shows ω_1's and the corresponding E for each beam.

4.3 GRAPHICAL PLOTS

Figures 11 and 12 are the calibration curves for strain gages and solar cell. For each case of the beams (Table 1) four plots corresponding to maximum

impact force, maximum strain, maximum deflection and impact duration have been drawn against the striking velocity V_o (Figs. 13 to 32). The non-dimensional maximum impact force ($\sigma_{max}^{3/2}$) and maximum strain (f_{max}) are plotted against impact parameter (λ) in Figures 33 and 34. To give an idea of the difference in the magnitude of forces and strains and their behaviour with respect to time for the two mathematical models 1 and 2, plots (figs. 35 and 36) are made for a particular case [Wt. of the striker = 2.92 lb ; V_o = 3.5 in/sec; beam used = beam 3A].

4.4 EFFECT OF IMPACT VELOCITY

Increment in impact velocity V_o increases the various quantities like impact force, strain, deflection as evident in Figures 11 to 32. The impact duration time has a tendency to become lower with increasing velocities as shown in Figures 16, 20, 24, 28, 32. Since in the mathematical model described in section 2.2 no energy is dissipated in the contact deformations, it is expected that force, deflection and strain should be greater as compared to those given by analysis in section 2.3 or the experiments. This is seen to be true from Figures 13 to 32 except for the case considered in Figures 13 and 17 which corresponds to Beam 1 and Beam 2 respectively. Thus it can be concluded that beam dimensions do effect the impact force as calculated

from eq.(2.2.26) for simply supported end conditions. And it can be said that for higher values of depth and height of the beam the results obtained from eq.(2.2.26) for the impact force are better. In the case of Figures 16, 20, 24, 28, 32 only the experimental values and those obtained from eq.(2.3.35) are plotted for comparison because it is obvious that in the first model the impact duration will be much less as shown in Figures 35, 36.

4.5 EFFECT OF BOUNDARY CONDITIONS

The effect of the boundary conditions on the various parameters was studied for the cases of Beam 1 and Beam 2. In Figures 13 and 17 the impact force obtained from eq.(2.2.26) is lower than the experimental values for simply supported and clamped boundaries. In the case of strain (figs. 14, 18) the experimental values for simply supported ends are very close to those corresponding to eq.(2.2.25) but for clamped ends, the experimental values are lower than those for simply supported beam showing the effect of boundary condition. Similarly in case of deflection the effect of boundaries is clear from Figures 15 and 19. In all the above cases the experimental values for simply supported beam are 20 to 40 percent higher than those for the clamped beam.

4.6 EFFECT OF PLASTIC DEFORMATION

This effect is found to be considerable in case of impact force. At low impact energies the experimental values of F_{max} are in the neighbourhood of the predicted ones, but in case of higher impact energies the experimental values show a remarkable deviation from the predicted values as seen in Figures 13, 17, 21, 25, 29. In the beginning with lower values of V_o, experimental curve has a tendency to follow the curve obtained from eq.(2.3.35) which takes into account the contact deformations [here force obtained from eq.(2.2.26) need not be compared because of the obvious deviations], but later for higher values of V_o the slope of experimental curve reduces. This decrement in the slope is mild in Beam 1, Beam 2 and Beam 3A but appreciable in Beam 3B and Beam 3C. This deviation may be attributed to the local plastic deformation. This shows that more accurate theoretical analysis is needed in the case of large impact velocities.

4.7 EFFECT OF IMPACT PARAMETER λ

Figures 33 and 34 show the dimensionless quantities $\bar{F}_{max}^{3/2}$ (maximum impact force) and f_{max} (maximum strain) plotted against the impact parameter λ respectively. For a particular configuration of beam and hammer, the value of λ depends upon the velocity V_o.

Both the predicted values and the experimental values have been compared. In case of Figure 34, the agreement is fairly good, but in Figure 33, at some stations the deviations are considerable. This may be attributed to the following reasons :

(a) The force indentation relation as given by eq.(2.1.2) is valid only for static compression of two isotropic elastic bodies. In dynamic case it may change.

(b) The relation (2.1.2) is valid for smooth curved surfaces. Even a little amount of inaccuracies involved in the fabrication of the hammer may change the value of K considerably.

(c) The supports cannot be ideal.

CHAPTER 5

CONCLUSIONS AND SUGGESTIONS FOR FURTHER WORK

5.1 CONCLUSION

The theory discussed in section 2.2 does not take into account the contact deformations and therefore it can be treated as more idealistic as compared to the other which considers the effects of contact deformations. The results obtained from it were also on the higher side as compared to those obtained from experiments or the other theory. Moreover it needed more computational efforts in calculating the second order derivatives with respect to time or x-coordinate. The trouble of convergence creeped in when the series was truncated at the fifth harmonic. If more than ten harmonics are considered the trouble of handling large quantities is encountered. Ultimately computation was done with only ten harmonics. In the case of simply supported beams the convergence was satisfactory, but for the clamped beam the situation was worse. However deflections in both the cases were obtained without any trouble.

The second theory (sec. 2.3) gives better results as well as the computational effort is also less. Finite difference technique for solving the

non-linear integral equation worked very satisfactorily. Moreover because of the dimensionless quantities involved in the computation, the job was simplified to a greater extent. Thus it can be concluded that the second theory which takes into account the contact deformations should be preferred for use in case of the transverse impact on beams inspite of the assumption that the impact is purely elastic.

For high velocities of impact a remarkable departure was obtained in case of the predicted results of impact force from the experimental values. This may be accounted to the limitation of the theory that nature of impact should be purely elastic. In the absence of this requirement the Hertz theory needs modifications in the calculation of the value of K, because it may not remain constant and may be influenced by the amount of indentations which occur in the beam. It is seen from the experimental results that the boundary conditions effect the beam response.

Instrumentation involved in the measurements of various parameters needs very careful attention. In the case of acceleration measurement, number of trials with various similar accelerometers were made to check their calibration and reliance for very high response. The response of the gage largely controlled by its

inertia, was assumed to be sufficiently high to permit the recording of the strains during impact the duration of which was about 200 micro seconds [20]. Using the solar cell for the measurement of deflection proved to be a very good and precise method in displacement measurement and also suitable for very high response because of the absence of any type of mechanical inertia effects.

5.2 SUGGESTIONS FOR FURTHER WORK

Regarding the analysis, improvement is possible if one takes into account the variation in the Hertz constant and the effect of permanent indentations in the two bodies. For example the force indentation relation can be expressed as

$$F(t) = K \left[w(t) - W_o \left(\frac{L}{2}, t \right) \right]^n \qquad (5.2.1)$$

where n in present work was 1.5.

Here the solutions may be investigated with the value of n other than 1.5. Instrumentation should be improved for very high impacts particularly in case of more rigid beams where the rise time of stresses or forces reduces to a very low value. Also the effect of multiple collisions should be studied. Attempts should be made to simplify the analysis to predict better results.

TABLE 1

LENGTH OF ALL BEAMS = 40.125"

No.	Beam Size D in.	H in.	ω rad/sec	ρ lb/in^3	E psi x 10^6	m_2 lb	Hammer radius in.
Beam 1	1.985	.483	174	.282	30.0	2.92	2
Beam 2	1.957	.955	130.5	.271	29.8	2.92	2
Beam 3A	1.995	.976	352	.283	30.5	2.92	2
Beam 3B	1.995	.976	352	.283	30.5	3.76	2
Beam 3C	1.995	.976	352	.283	30.5	8.95	3

TABLE 2

Beam 1. DATA : $\rho = .282$ lb/in^3, D = 1.985 in,
H = .483 in., E = 30×10^6 psi, m_2 = 2.92 lb,
m_1 = 10.85 lb, M = 3.72, α = 3.3911 lb^{-1}in.sec$^{-3/2}$,
K = $.3105 \times 10^8$ lb in.$^{-3/2}$, ν = .3

V_o in/sec.	$T \times 10^{-6}$ sec.	λ	$\sigma_{max.}^{3/2}$	$(KTV_o)^{3/2}$	$f_{max}(\lambda)$	Exp. $\sigma_{max.}^{3/2}$	Exp. $f_{max.}$
7	96.711	2.606	.412	547	.623	.522	.750
14	84.194	2.792	.396	1255	.591	.460	.646
17.5	80.521	2.855	.391	1640	.582	.412	.628
21	77.640	2.908	.386	2045	.574	.351	.650
28	73.304	2.993	.380	2880	.561	.375	.615

TABLE 3

Beam 2. DATA : ρ = .282 lb/in.^{3}, D = 1.957 in., H = .355 in, E = 29.8 x 10^6 psi, m_2 = 2.92 lb., m_1 = 7.55 lb., M = 2.59, α = 3.4453 $lb^{-1}in.sec^{-3/2}$, K = .308 x 10^8 $lb.in^{-3/2}$, ν = .3

V_o in/sec.	$Tx10^{-6}$ sec.	λ	$\sigma_{max.}^{3/2}$	$K(TV_o)^{3/2}$	$f_{max}(\lambda)$	Exp. $\sigma_{max.}^{3/2}$	Exp f_{max}
3.5	110.300	4.030	.315	240	.441	.400	.600
7	96.070	4.318	.300	550	.416	.436	.466
10.5	88.600	4.497	.292	895	.402	.322	.415
14	83.640	4.630	.286	1265	.392	.285	.434
17.5	79.990	4.730	.282	1655	.385	.267	.407

TABLE 4

Beam 31. DATA : ρ = .283 lb./in.^{3}, D = 1.995 in., H = .976 in., E = 30x10^6 psi, α = .013387 lb^{-1}in.sec$^{-3/2}$, ν = .3, m_1 = 22.2 lb, m_2 = 2.92 lb., M = 7.6, K = .3157x10^8 lb in.$^{-3/2}$

V_o in/sec.	Tx10^{-6} sec.	λ	$\sigma^{3/2}_{max.}$	$K(TV_o)^{3/2}$	$f_{max}(\lambda)$	Exp. $\sigma^{3/2}_{max}$	Exp. $f_{max.}$
3.5	110.360	.840	.709	240	1.222	.846	1.480
7	96.070	.899	.690	551	1.184	.590	1.380
10.5	88.590	.937	.680	895	1.162	.458	1.352
14	83.640	.964	.673	1265	1.147	.363	1.342
17.5	79.990	.986	.667	1654	1.135	.320	1.355

TABLE 5

Beam 3B. DATA : ρ = .283 lb./in.^{3}, D = 1.995 in., H = .976 in., E = 30×10^6 psi, α = .013387 $lb^{-1} in. sec.^{-3/}$ ν = .3, m_1 = 22.2 lb., m_2 = 3.76 lb., M = 5.9, K = $.3157 \times 10^8$ lb. $in.^{-3/2}$

V_o in/sec.	$T \times 10^{-6}$ sec.	λ	$\sigma_{max}^{3/2}$	$K(TV_o)^{3/2}$	$f_{max}(\lambda)$	$\sigma_{max}^{Exp.\,3/2}$	$f_{max}^{Exp.}$
3.5	121.190	1.025	.657	278	1.114	.947	1.532
7	106.180	1.099	.639	642	1.075	.577	1.255
10.5	97.92	1.144	.628	1040	1.052	.564	1.262
14	92.44	1.178	.620	1470	1.036	.442	1.253
17.5	88.4	1.204	.614	1920	1.0236	.402	1.175

TABLE 6

Beam 3C. DATA : ρ = .283 lb./in.^{3}, D = 1.995 in., H = .976 in., E = 30x10^6 psi, α = .013387 lb^{-1}in.sec$^{-3/2}$, ν = .3, m_1 = 22.2 lb., m_2 = 8.95 lb., M = 2.48, K = .387 x 10^8 lb.in.$^{-3/2}$

V_o in/sec.	$Tx10^{-6}$ sec.	λ	$\sigma_{max}^{3/2}$	$K(TV_o)^{3/2}$	$f_{max}(\lambda)$	Exp. $\sigma_{max}^{3/2}$	Exp. f_{max}
3.5	159.300	2.140	.461	510	.717	.871	1.398
7	138.660	2.295	.443	1171	.684	.504	.923
10.5	127.860	2.389	.433	1900	.664	.388	.821
14	120.720	2.459	.425	2690	.650	.306	.793
17.5	115.450	2.515	.420	3510	.639	.253	.720

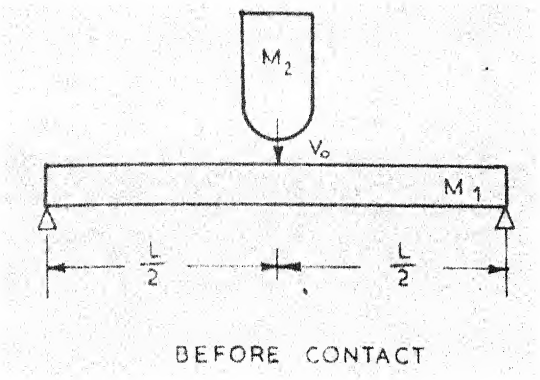
M2
Vo
M1
L/2
L/2
BEFORE CONTACT

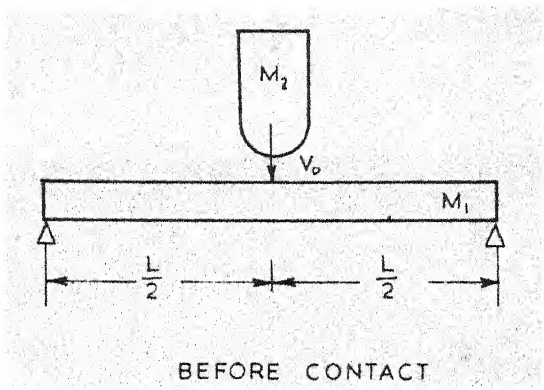
M2
Vo
M1
L/2
L/2
BEFORE CONTACT

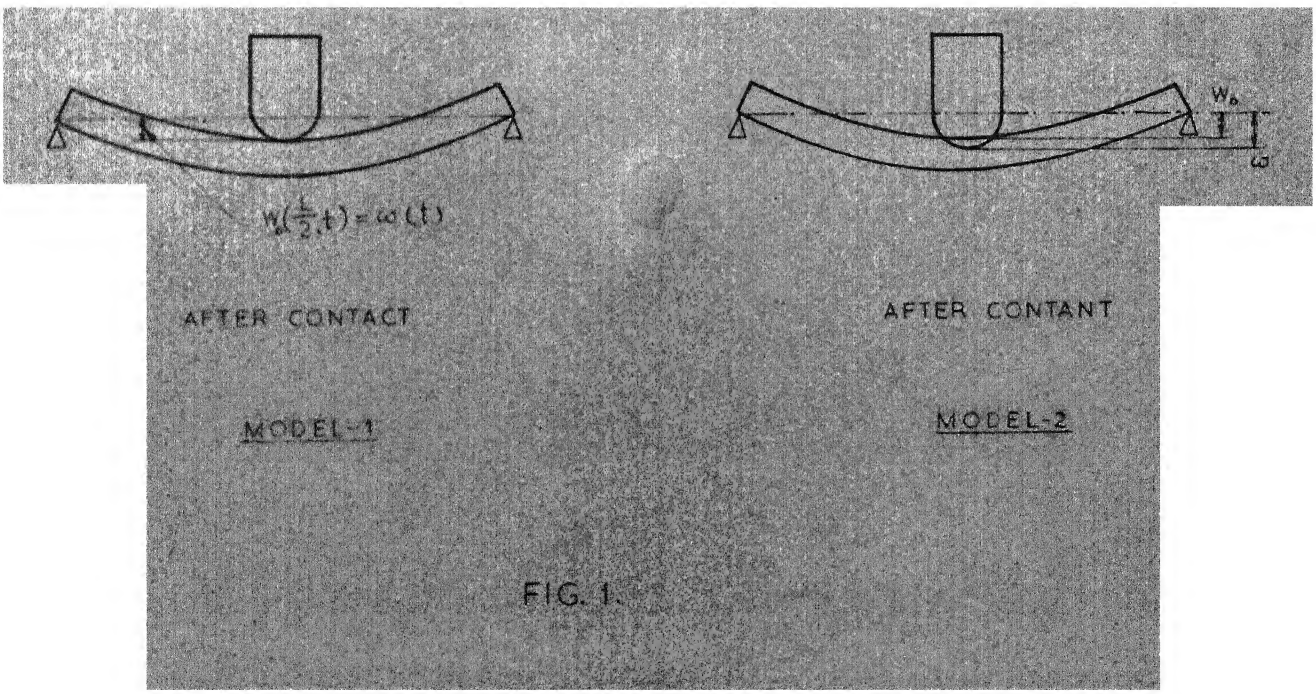
W(L/2,t) = ω(t)
AFTER CONTACT
MODEL-1
AFTER CONTANT
MODEL-2

FIG. 1.

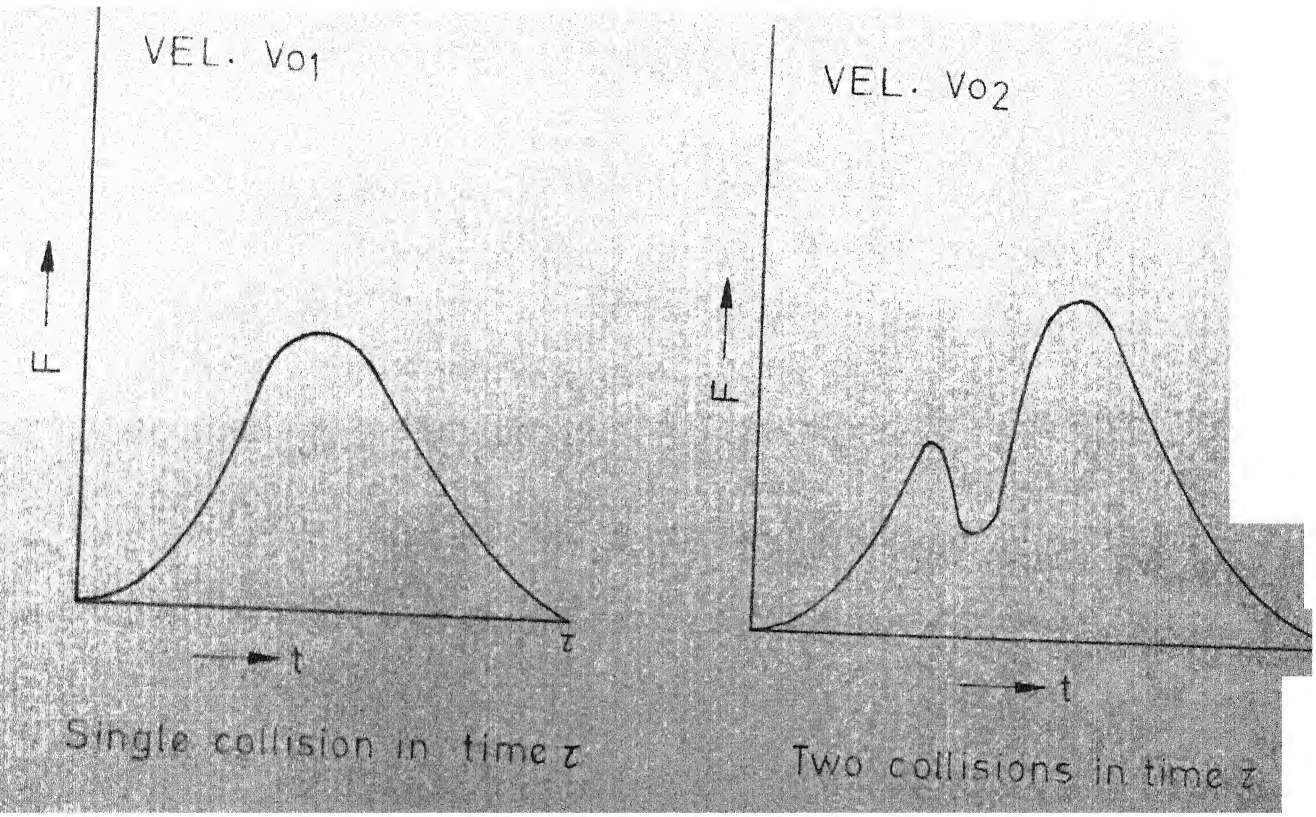

FIG. 2 EFFECT OF VELOCITY ON COLLISION PHENOMENON
($V_{o2} > V_{o1}$)

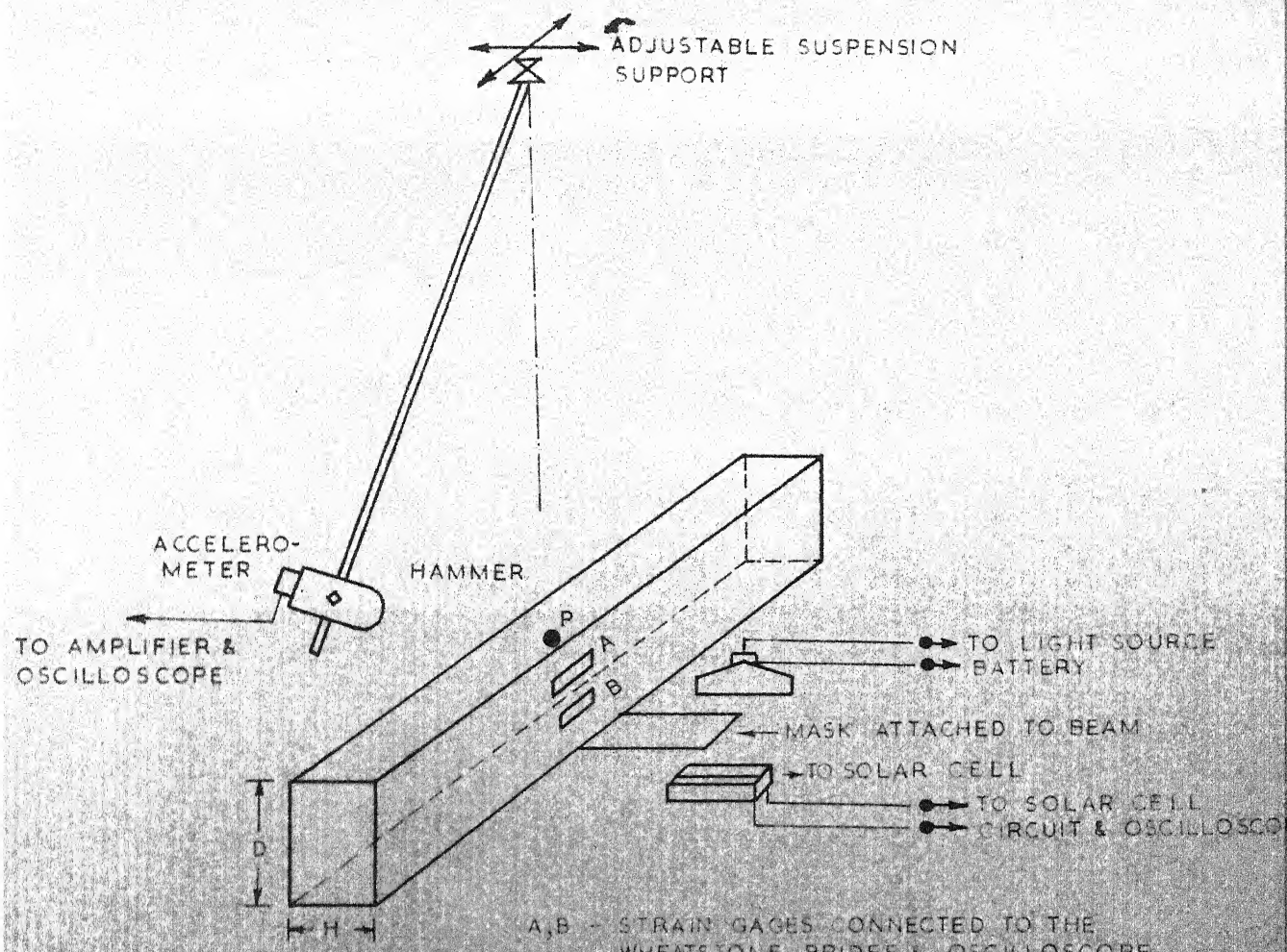

FIG.3. LINE SKETCH FOR EXPERIMENTAL ARRANGEMENT.

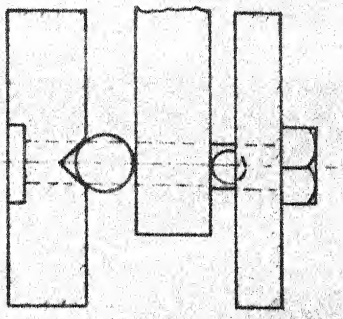

SECTION A-A

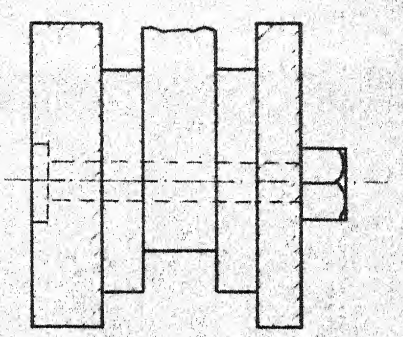

SECTION A-A

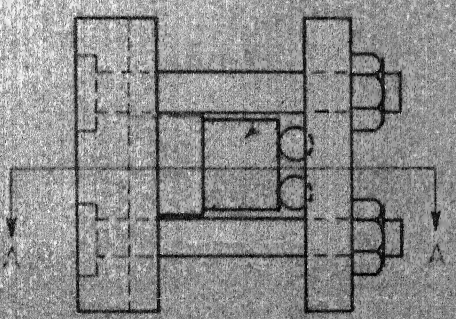

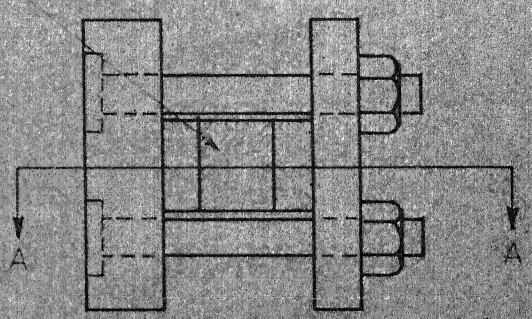

FIG. 4 SIMPLE SUPPORT

FIG. 5 CLAMP SUPPORTS

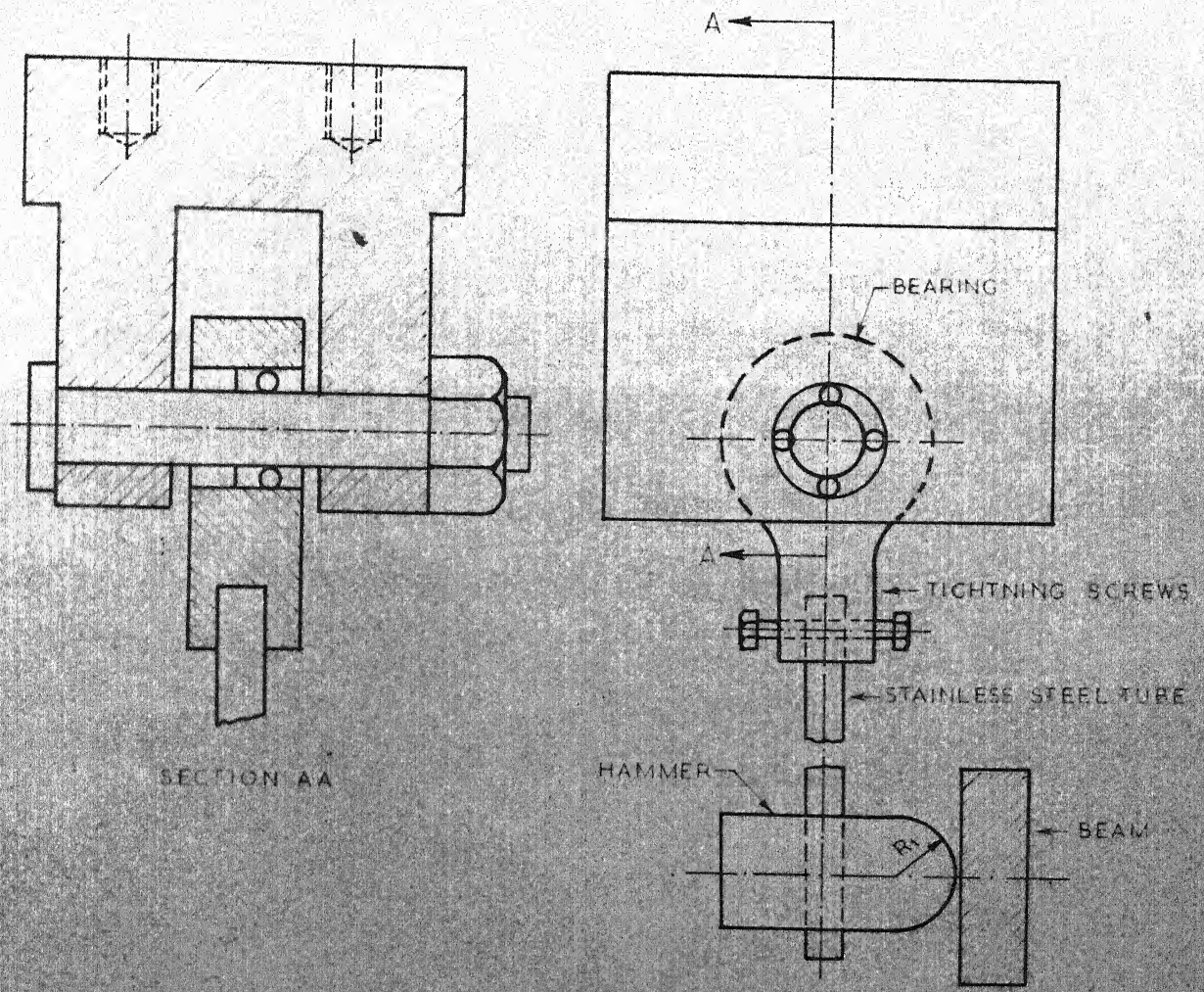
A
BEARING
A
TIGHTNING SCREWS
STAINLESS STEEL TUBE
HAMMER
BEAM
SECTION AA

FIG. 6.

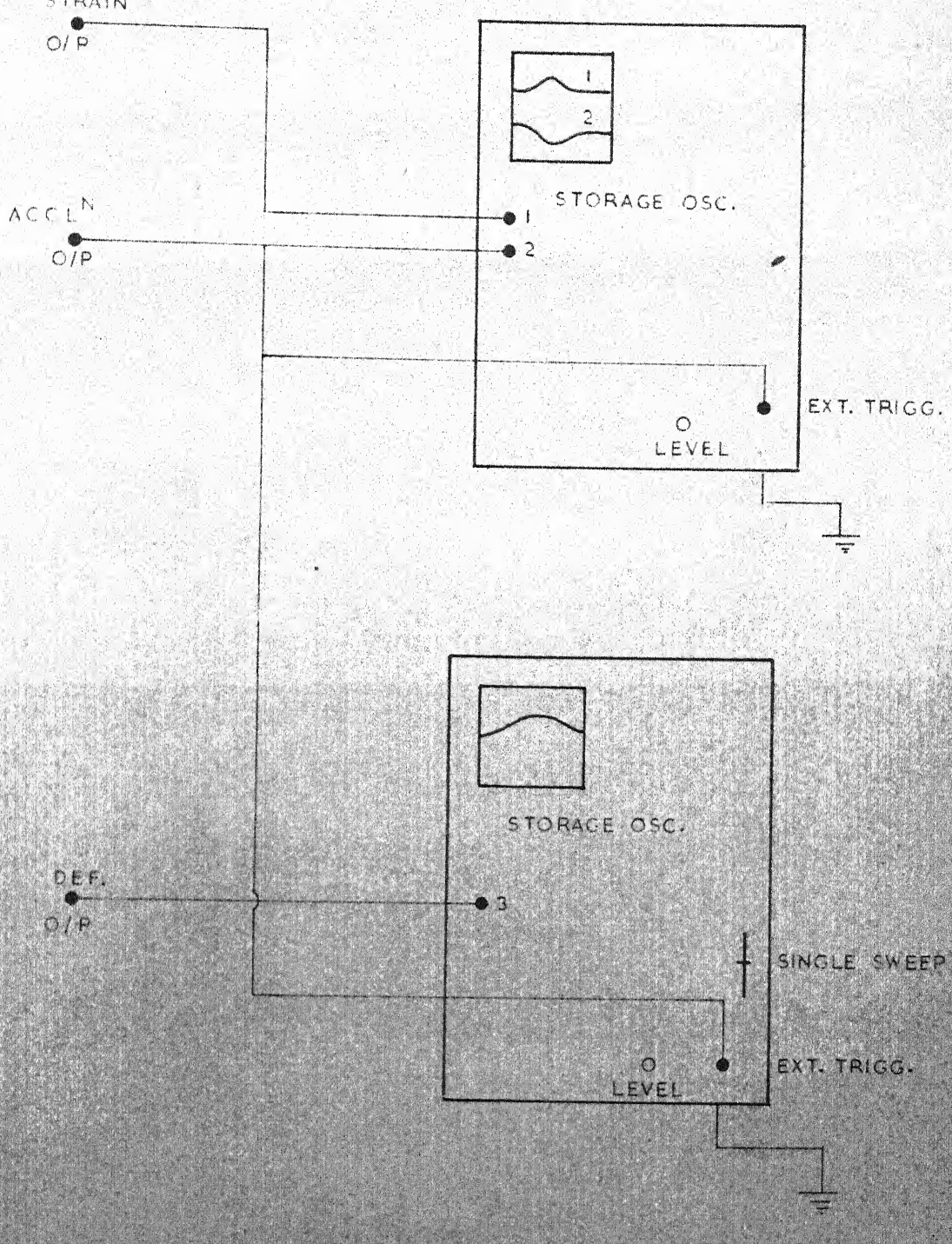

FIG. 7. LINE SKETCH FOR INPUT RECORDING AND OSCILLOICOPES TRIGGERING.

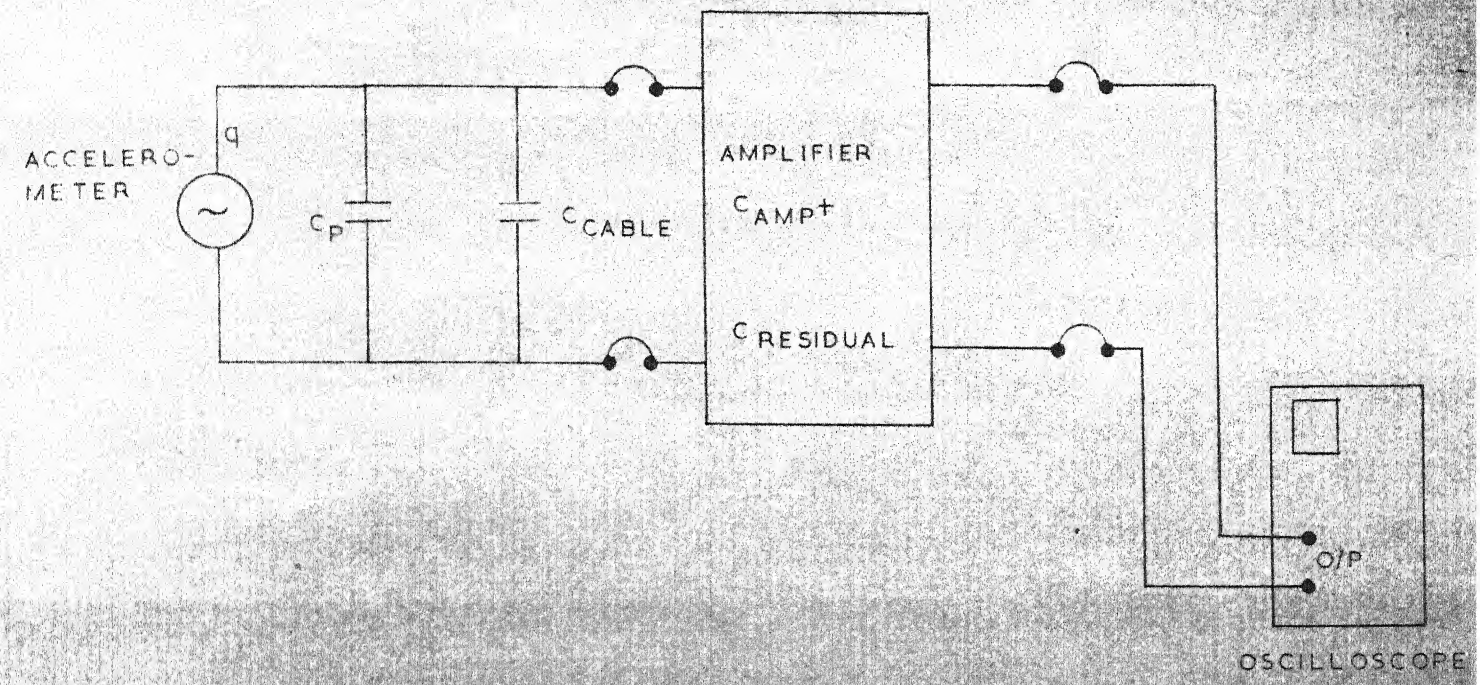

FIG 8 ACCELEROMETER CIRCUIT

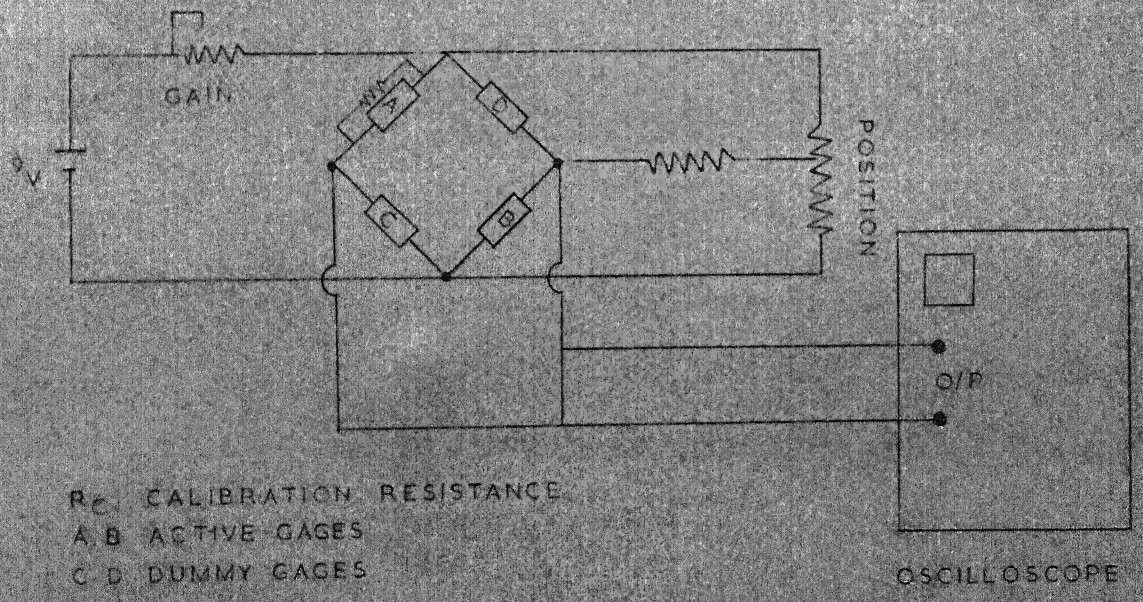

R_c CALIBRATION RESISTANCE
A B ACTIVE GAGES
C D DUMMY GAGES

FIG. 9 STRAIN GAGE CIRCUIT

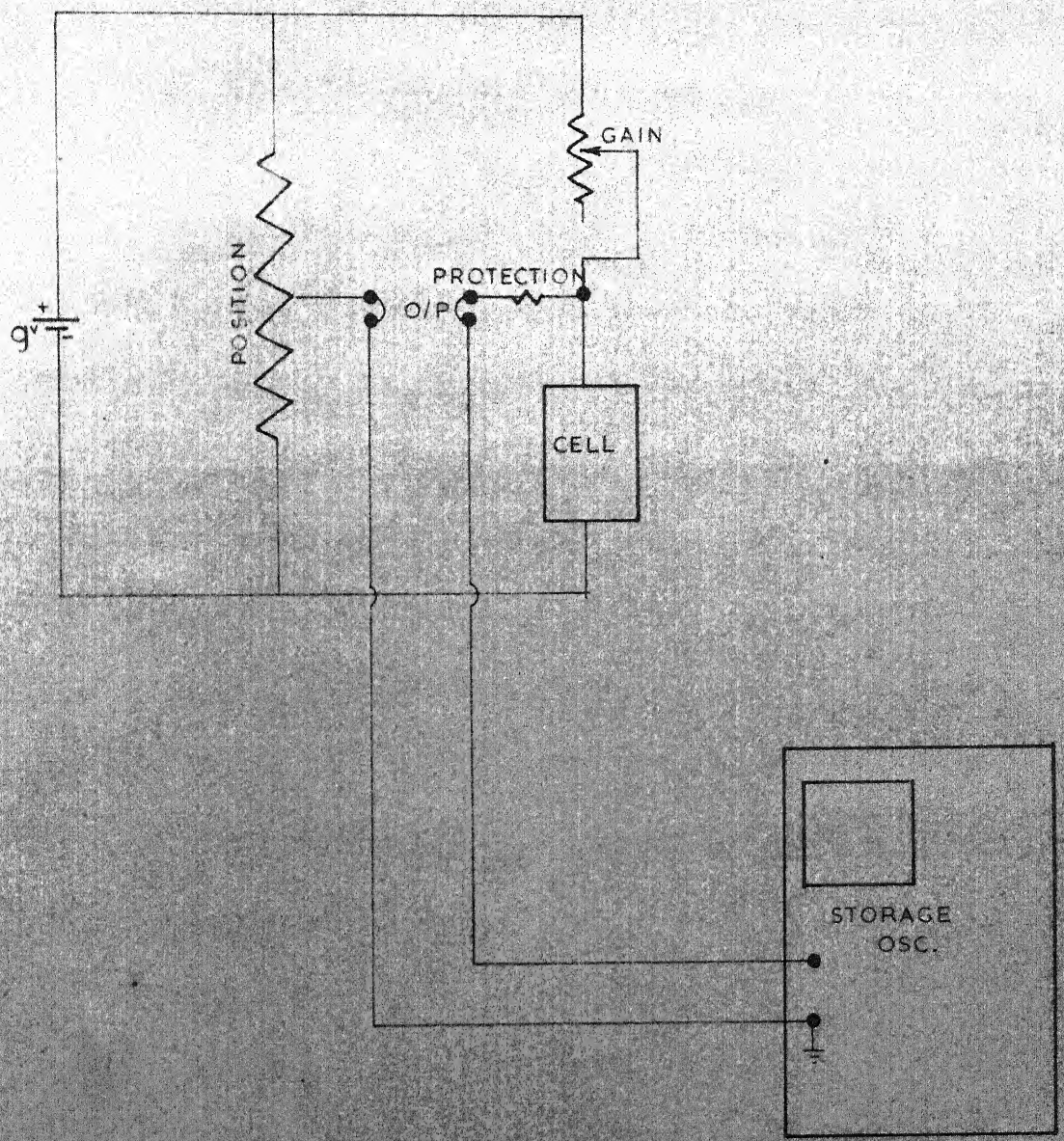

FIG.10. SOLAR CELL DISPLACEMENT TRANIDUCER CIRCUIT.

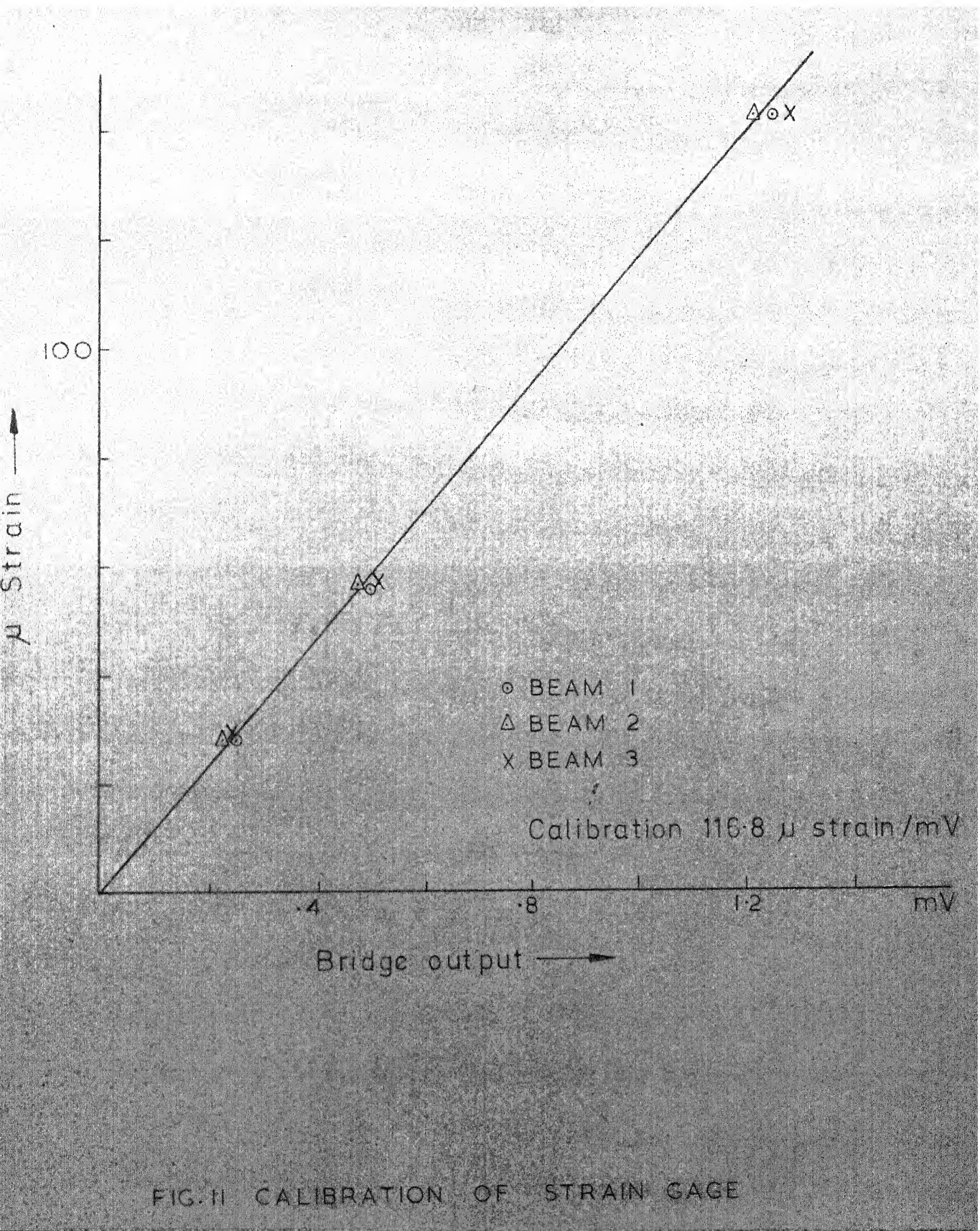

FIG. 11 CALIBRATION OF STRAIN GAGE

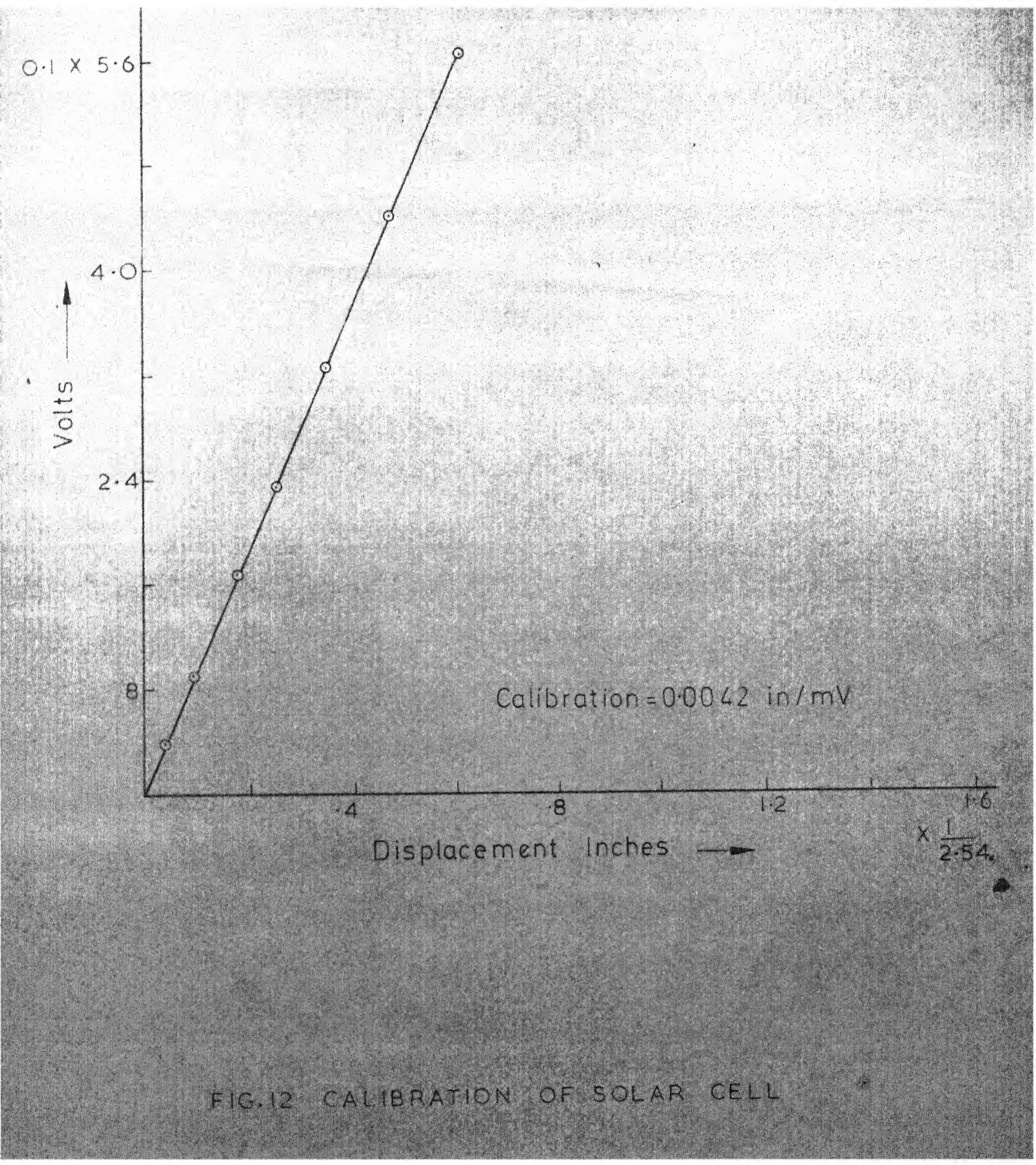

FIG. 12 CALIBRATION OF SOLAR CELL

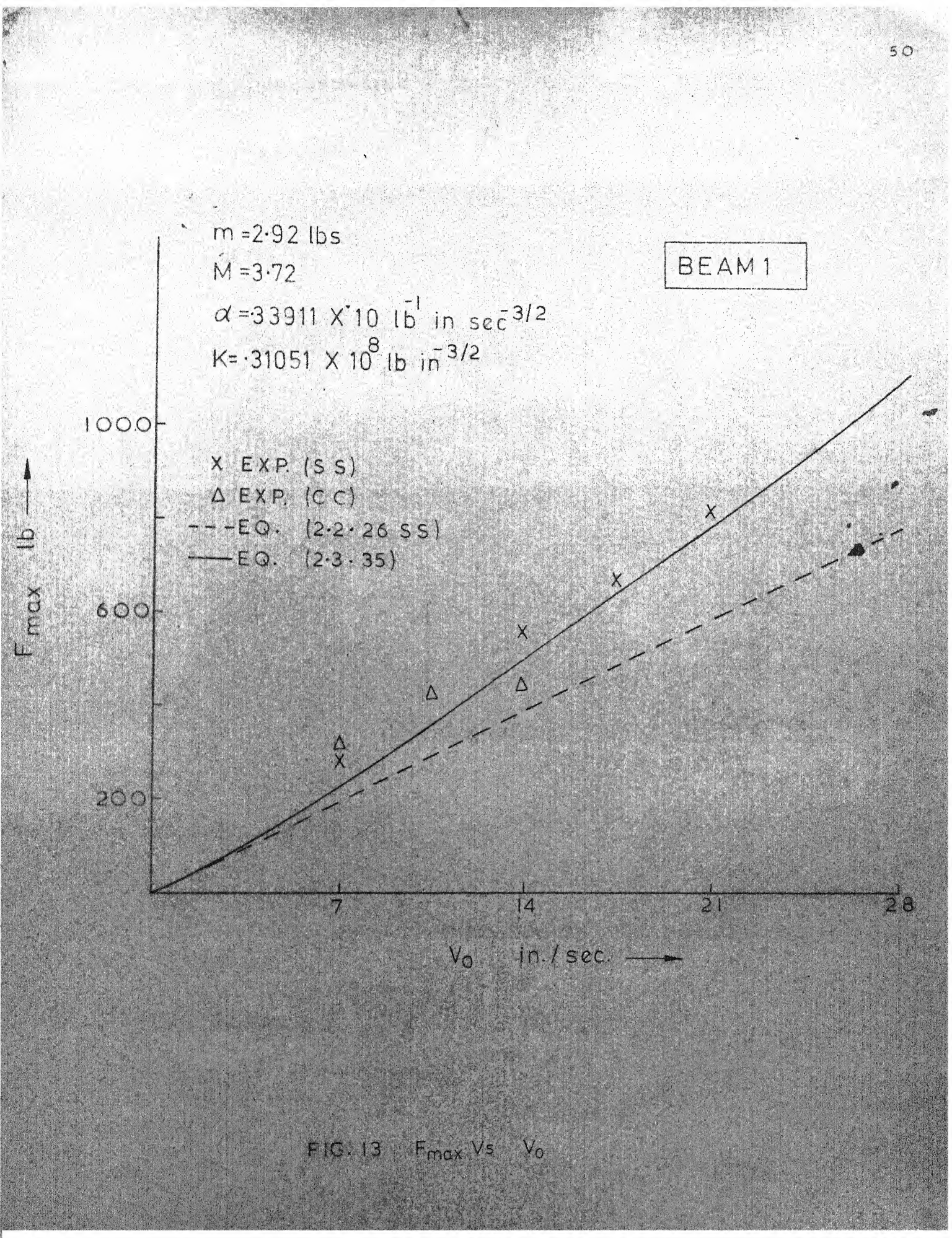

FIG. 13 F_{max} Vs V_0

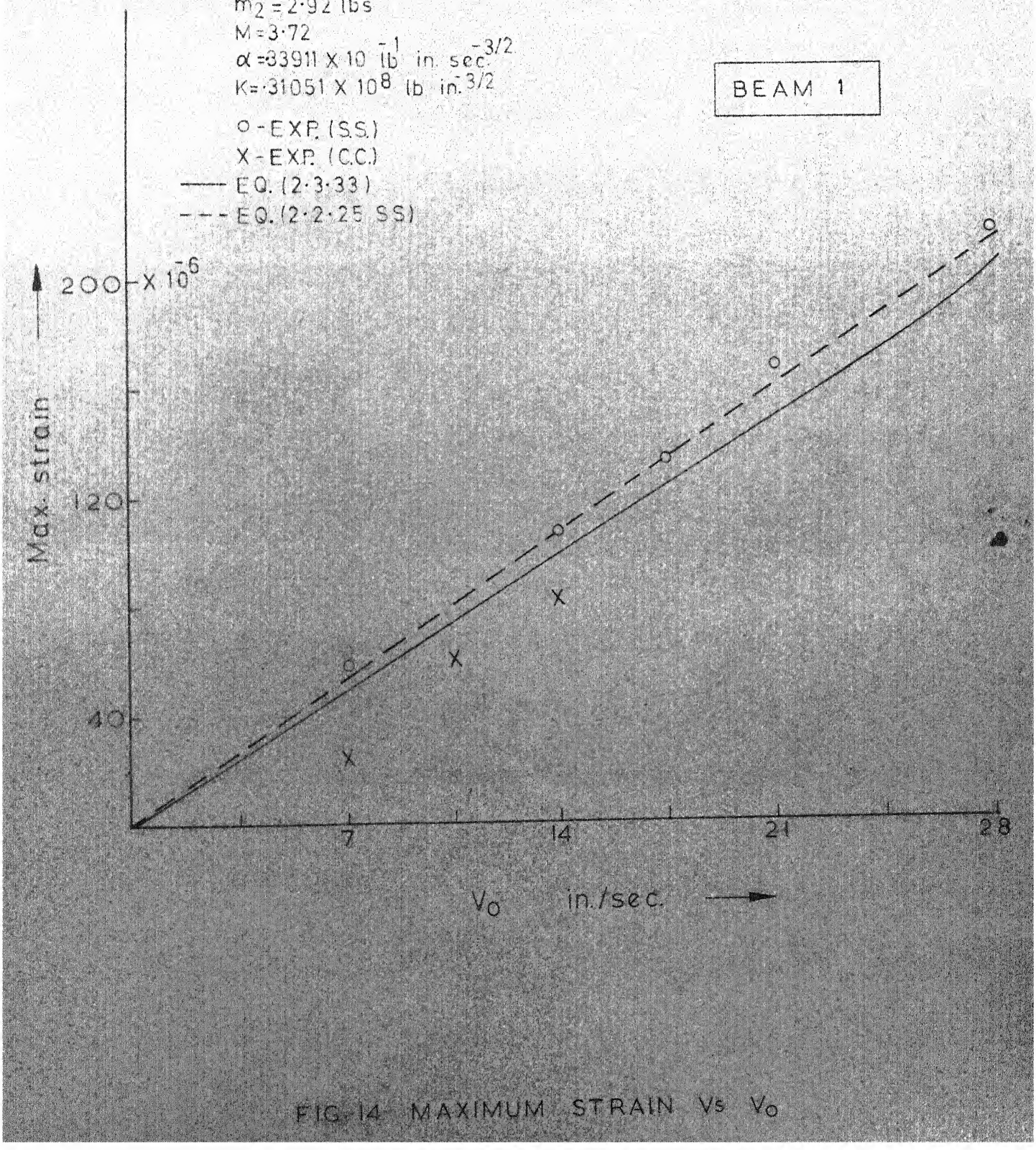

FIG. 14 MAXIMUM STRAIN Vs V_o

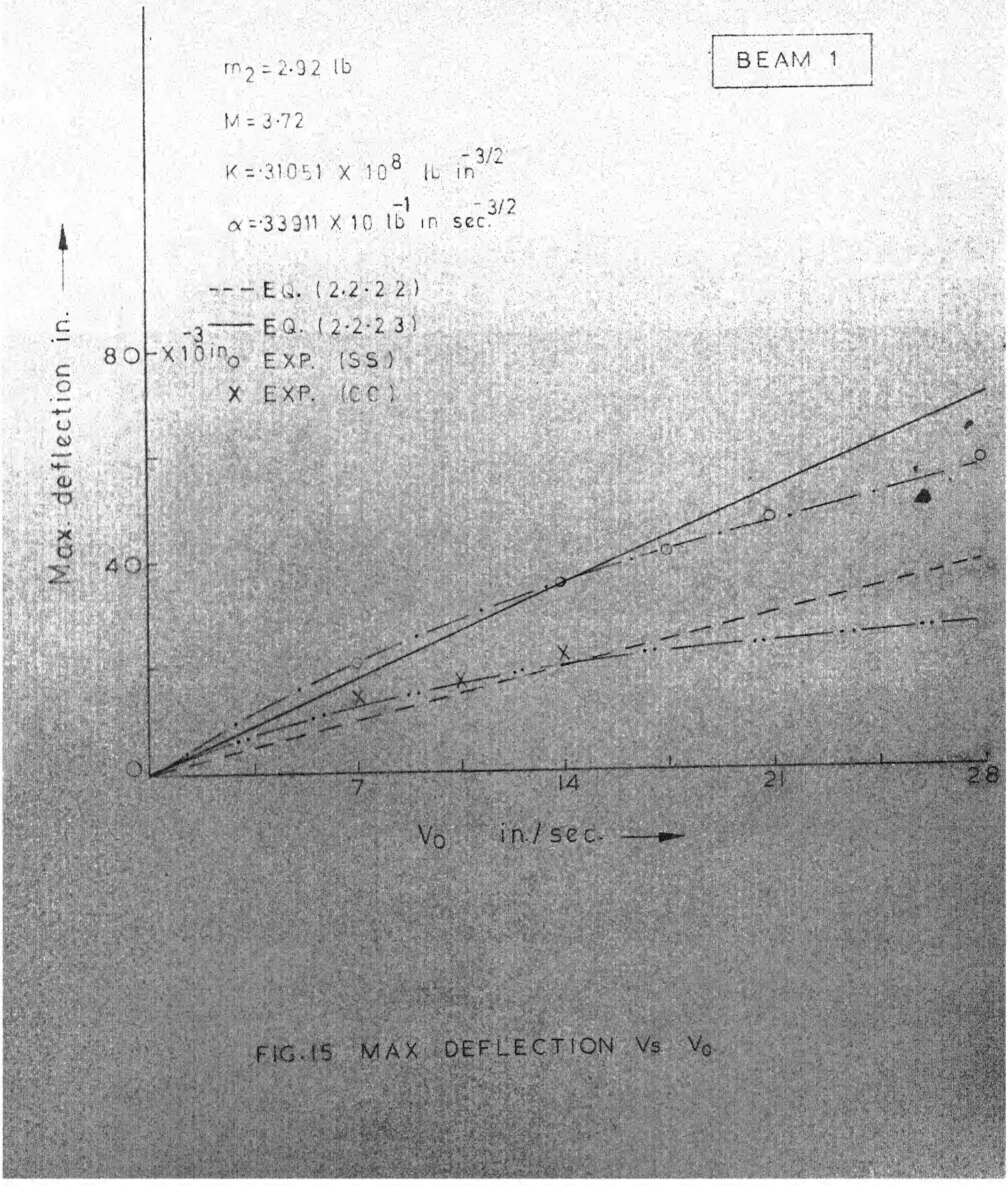

FIG.15 MAX DEFLECTION Vs V_o

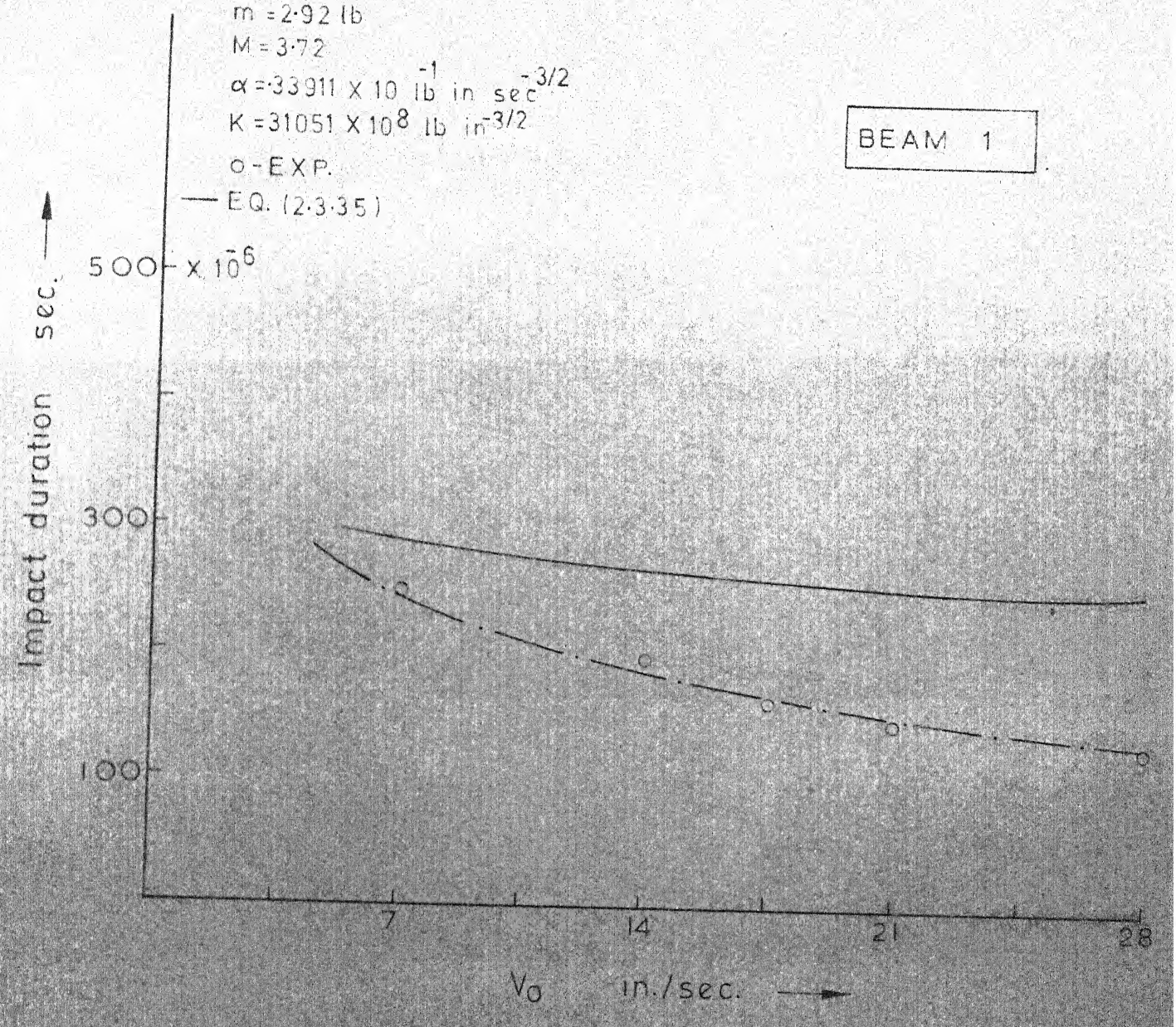

FIG. 16 IMPACT DURATION Vs V_0

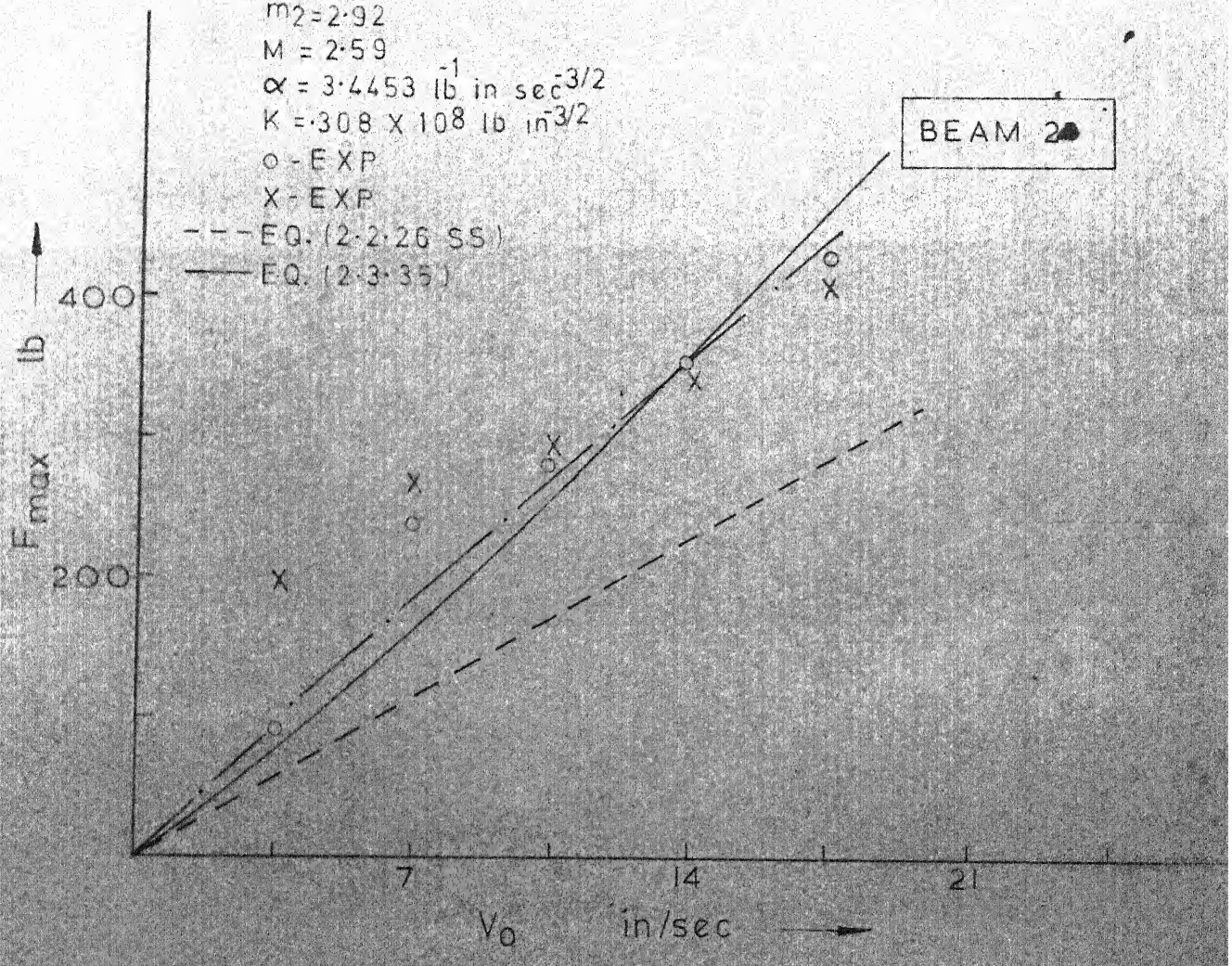

FIG. 17 Fmax Vs V0

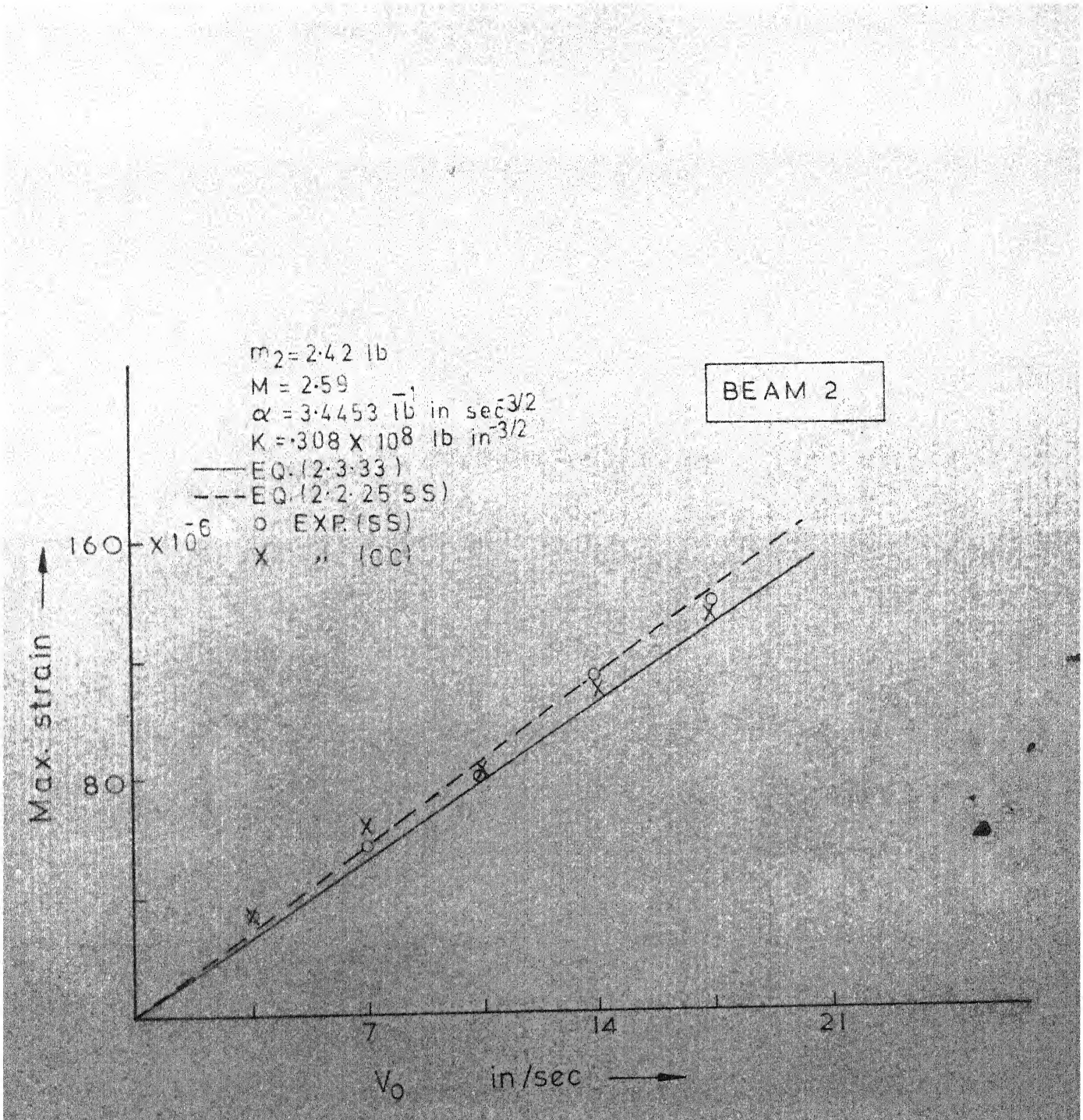

FIG. 18 MAX STRAIN Vs V_o

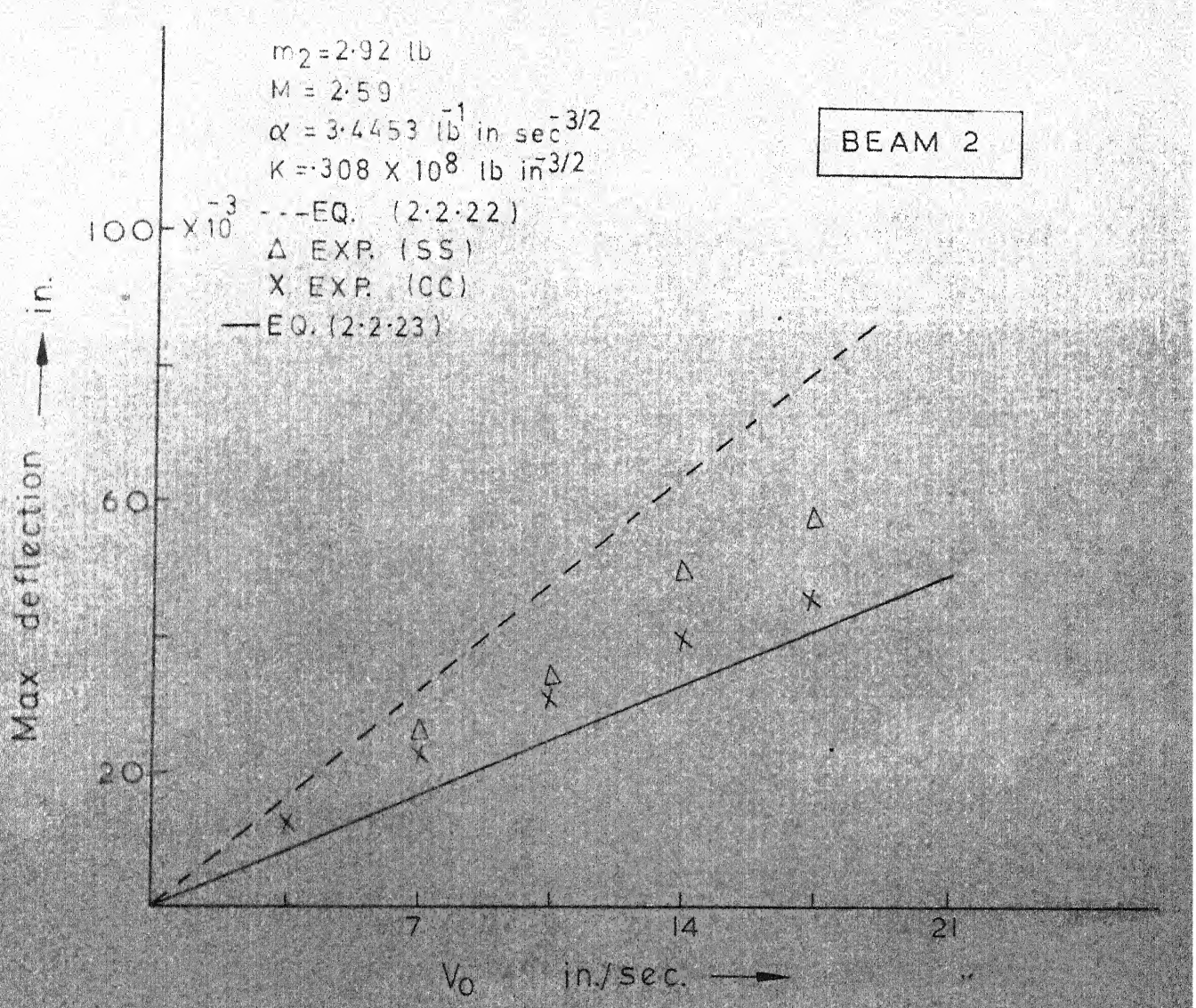

FIG. 19 MAX. DEFLECTION Vs V_0

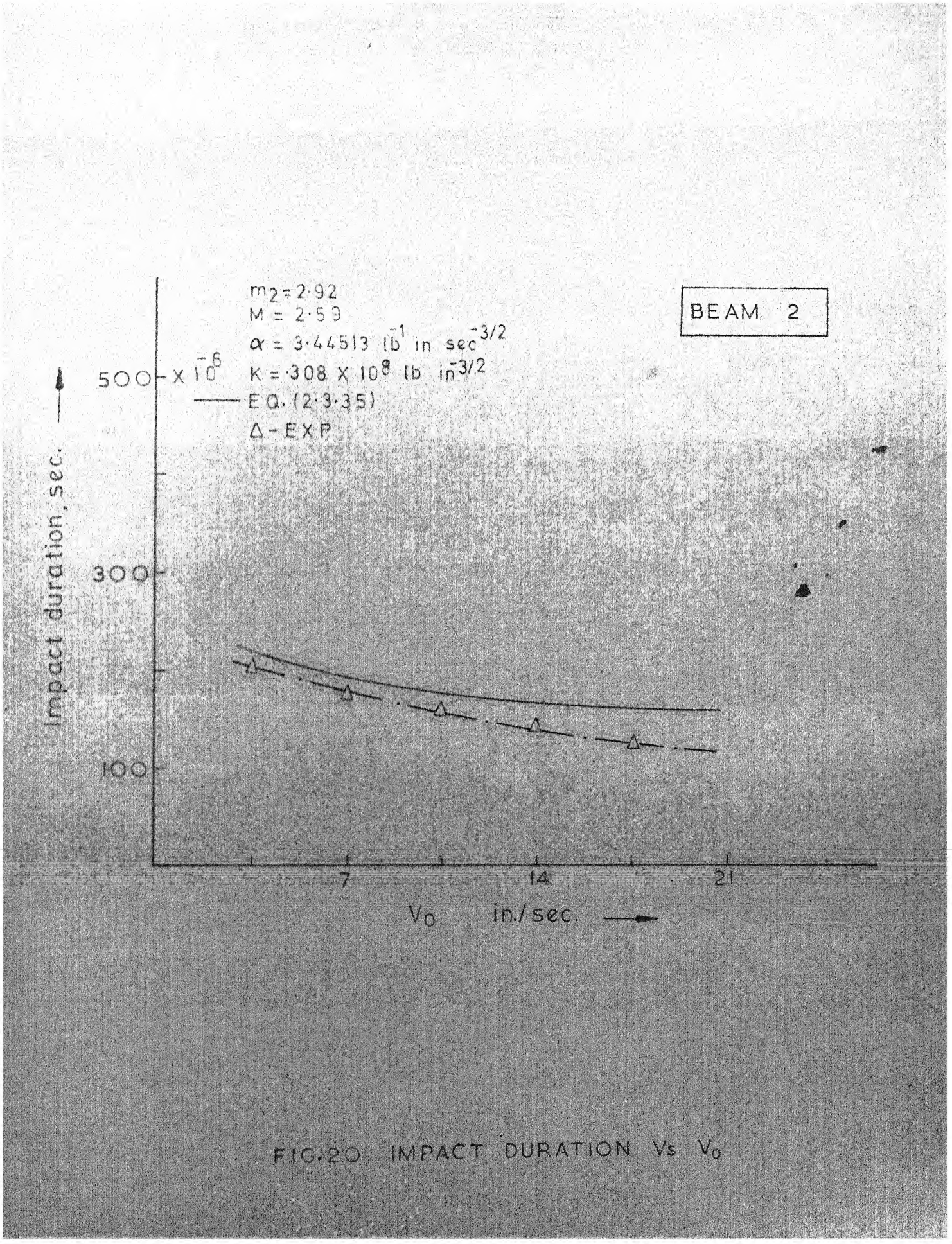

FIG.20 IMPACT DURATION Vs V_0

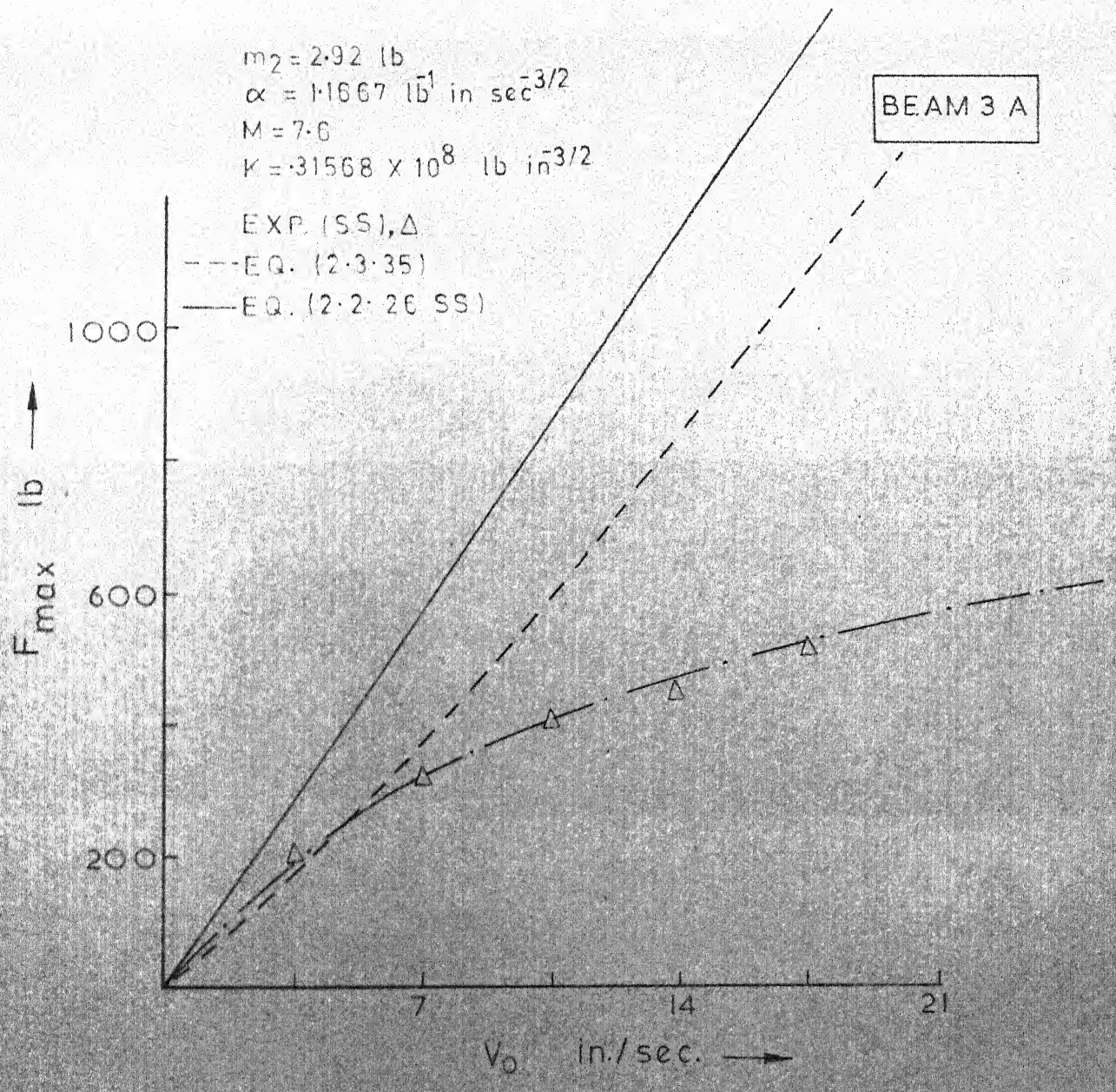

FIG. 21 F_{max} Vs V_0

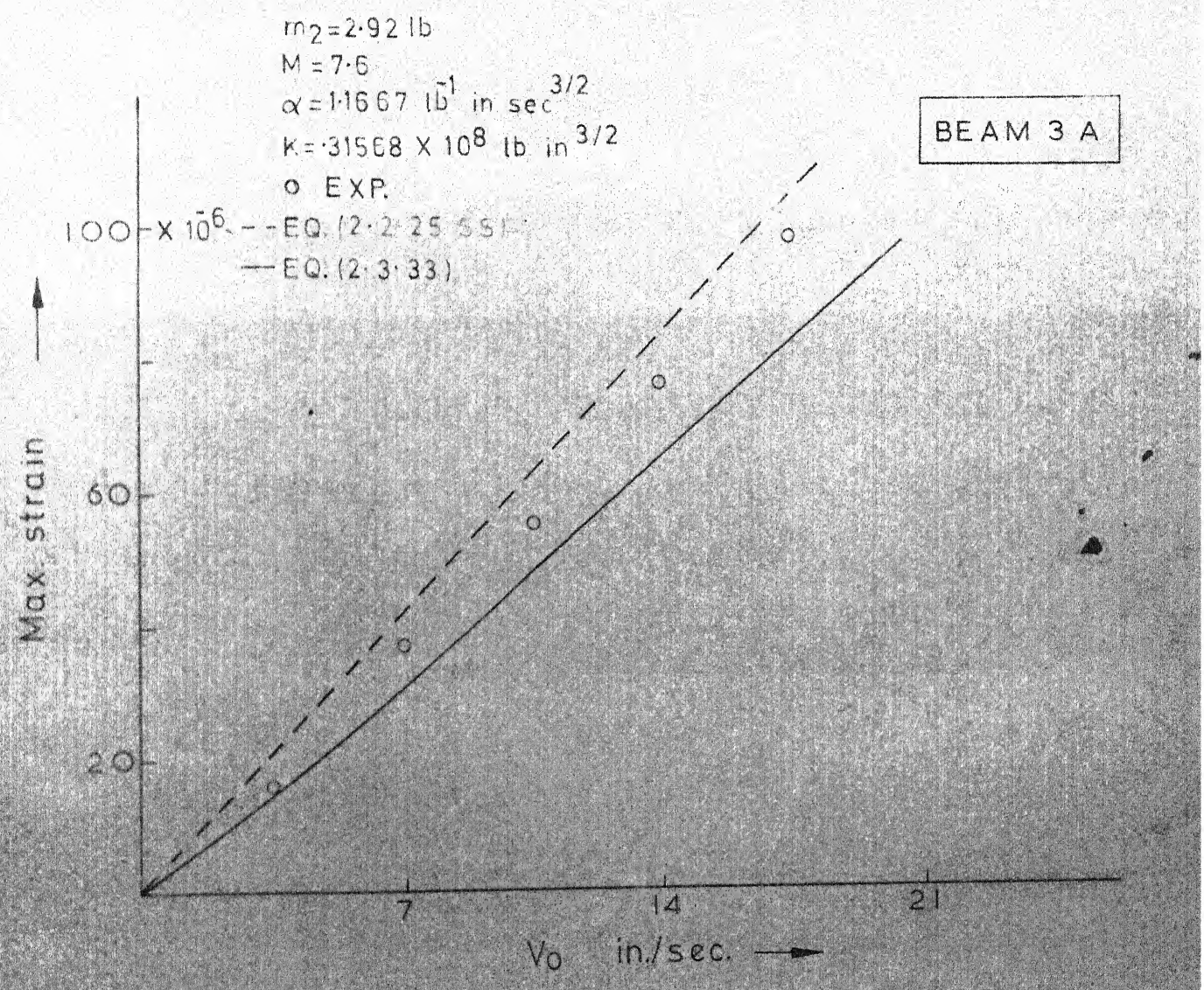

FIG.22 MAX. STRAIN Vs V_0

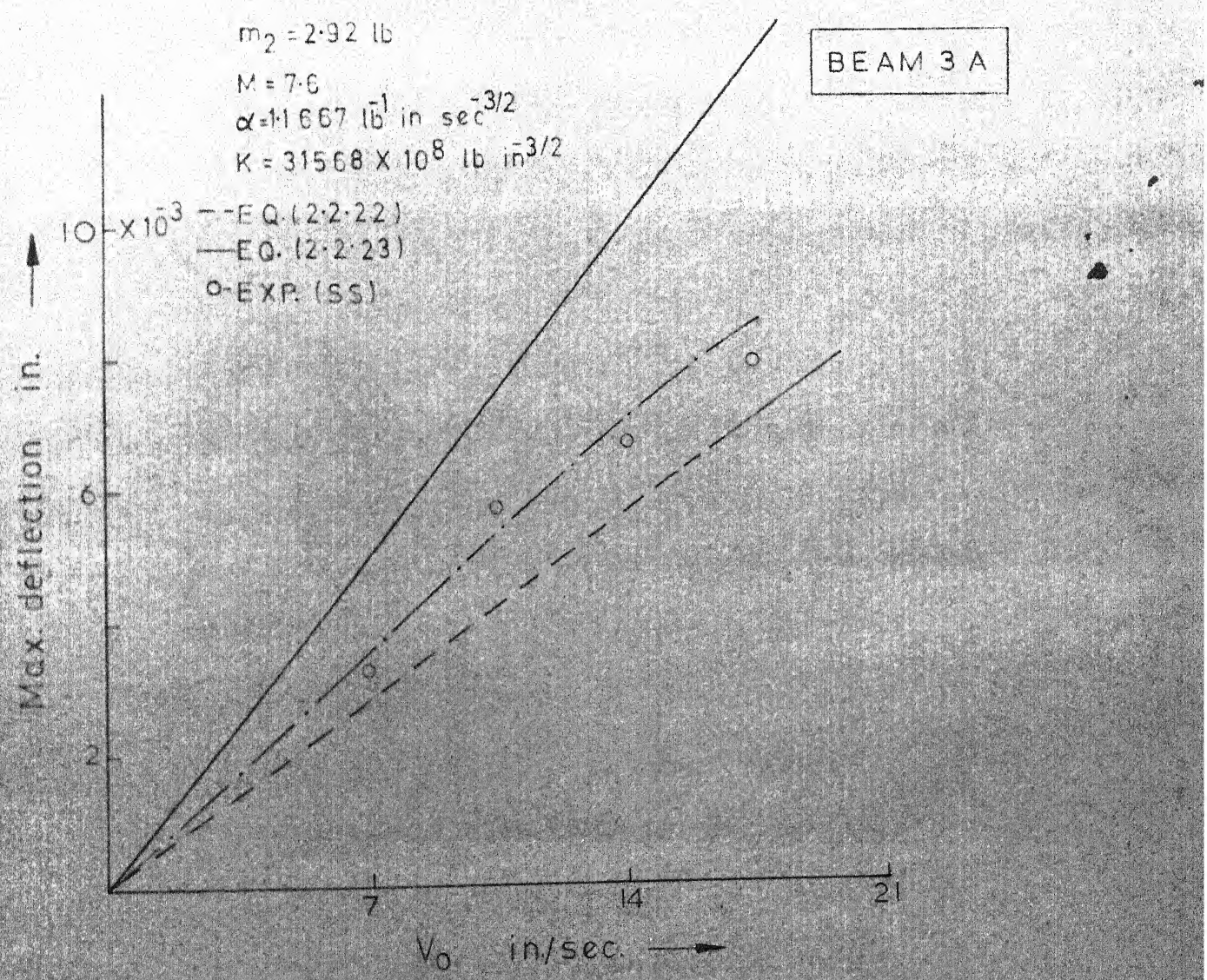

FIG. 23 MAX. DEFLECTION Vs V_0

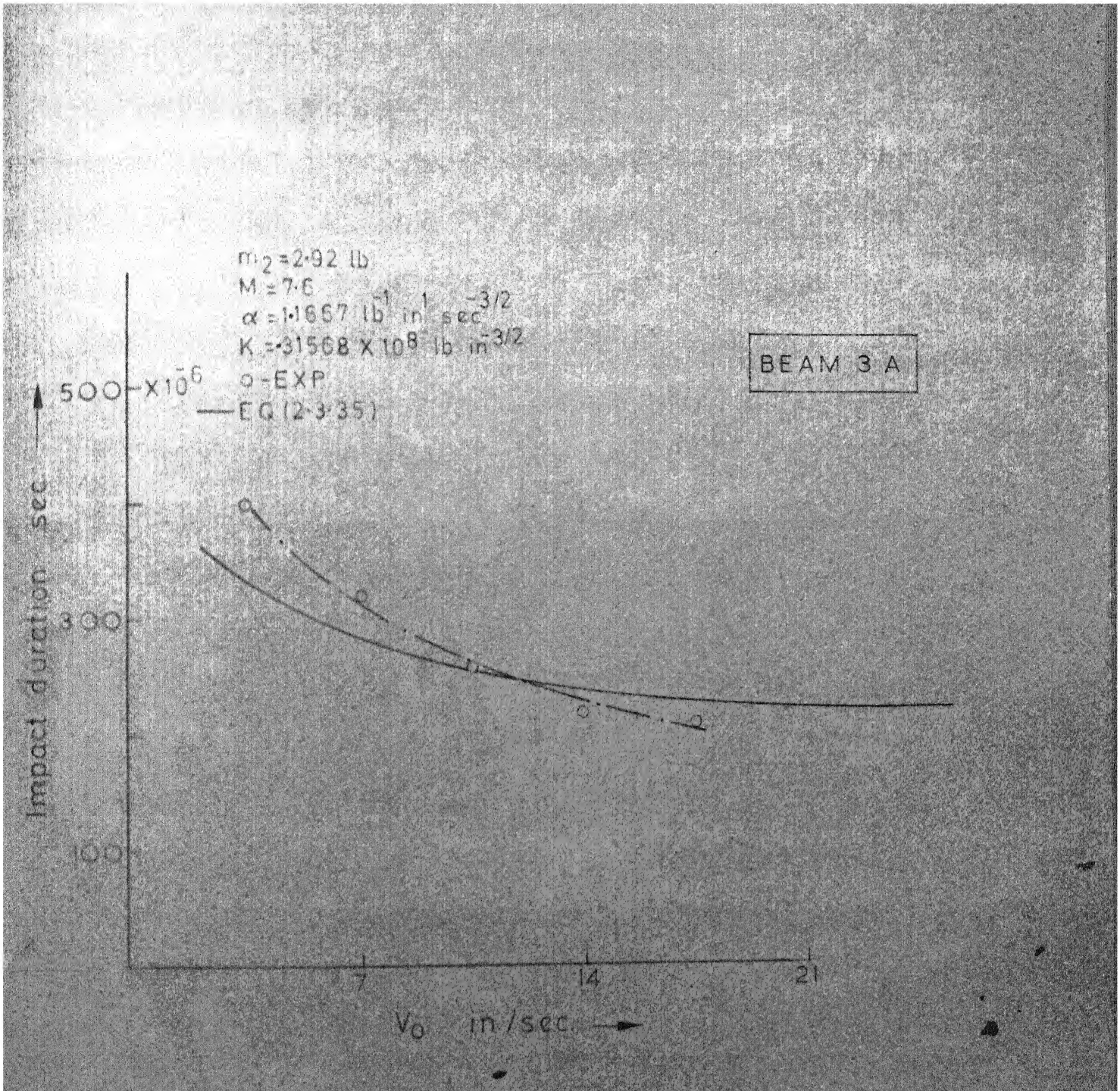

FIG 24 IMPACT DURATION Vs V_0

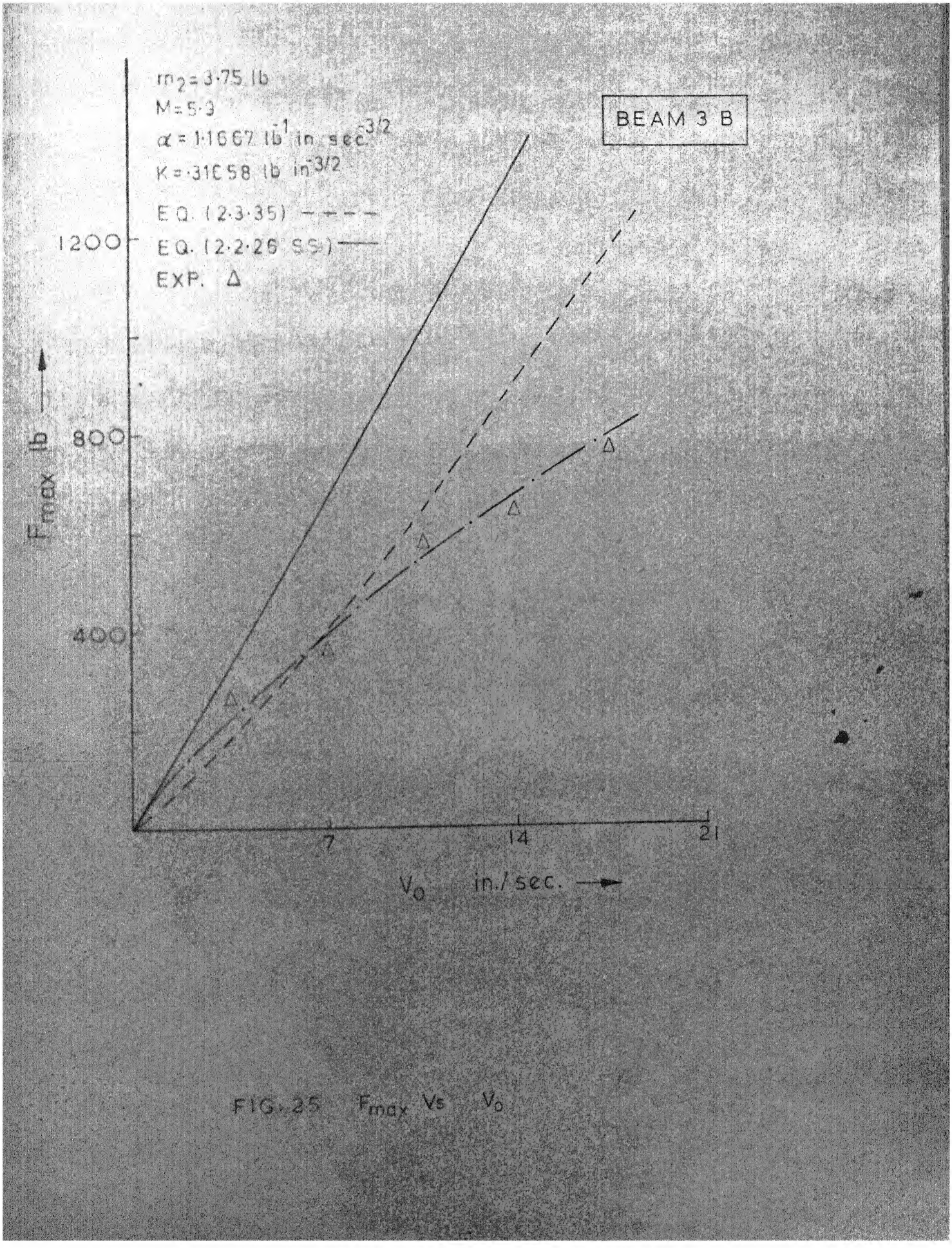

FIG. 25 F_{max} Vs V_0

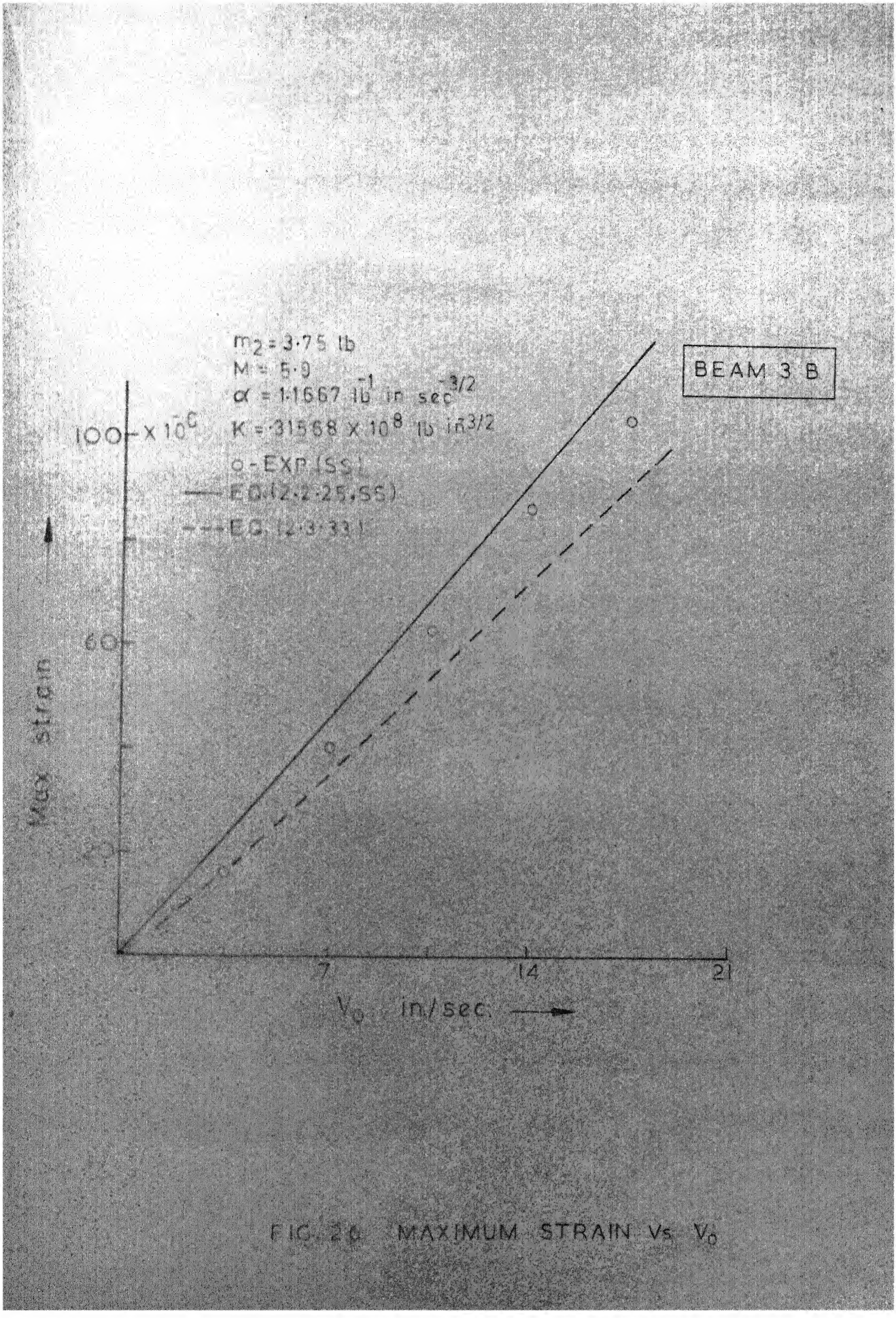

FIG. 2.0 MAXIMUM STRAIN Vs V_0

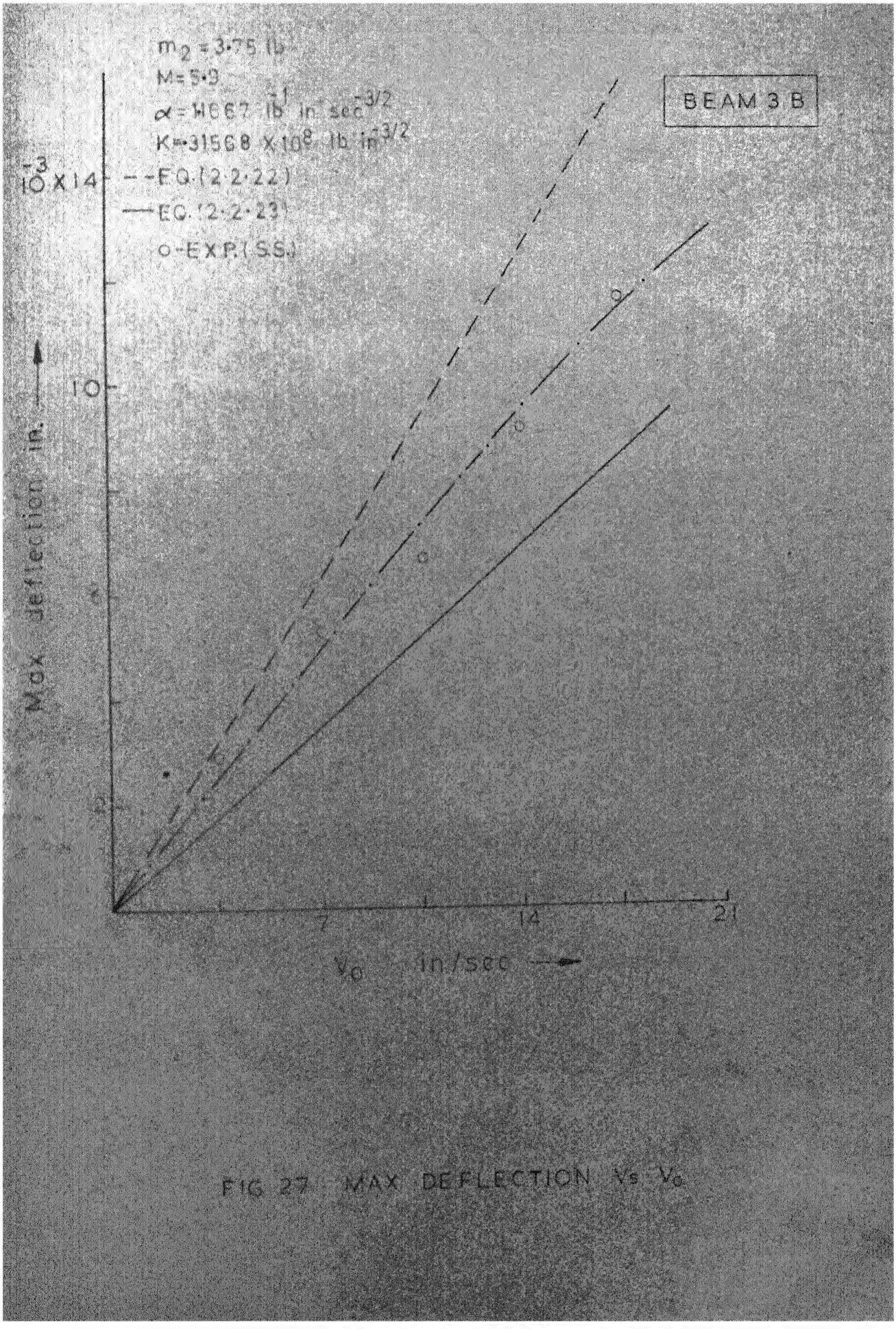

FIG 27 MAX DEFLECTION Vs V_0

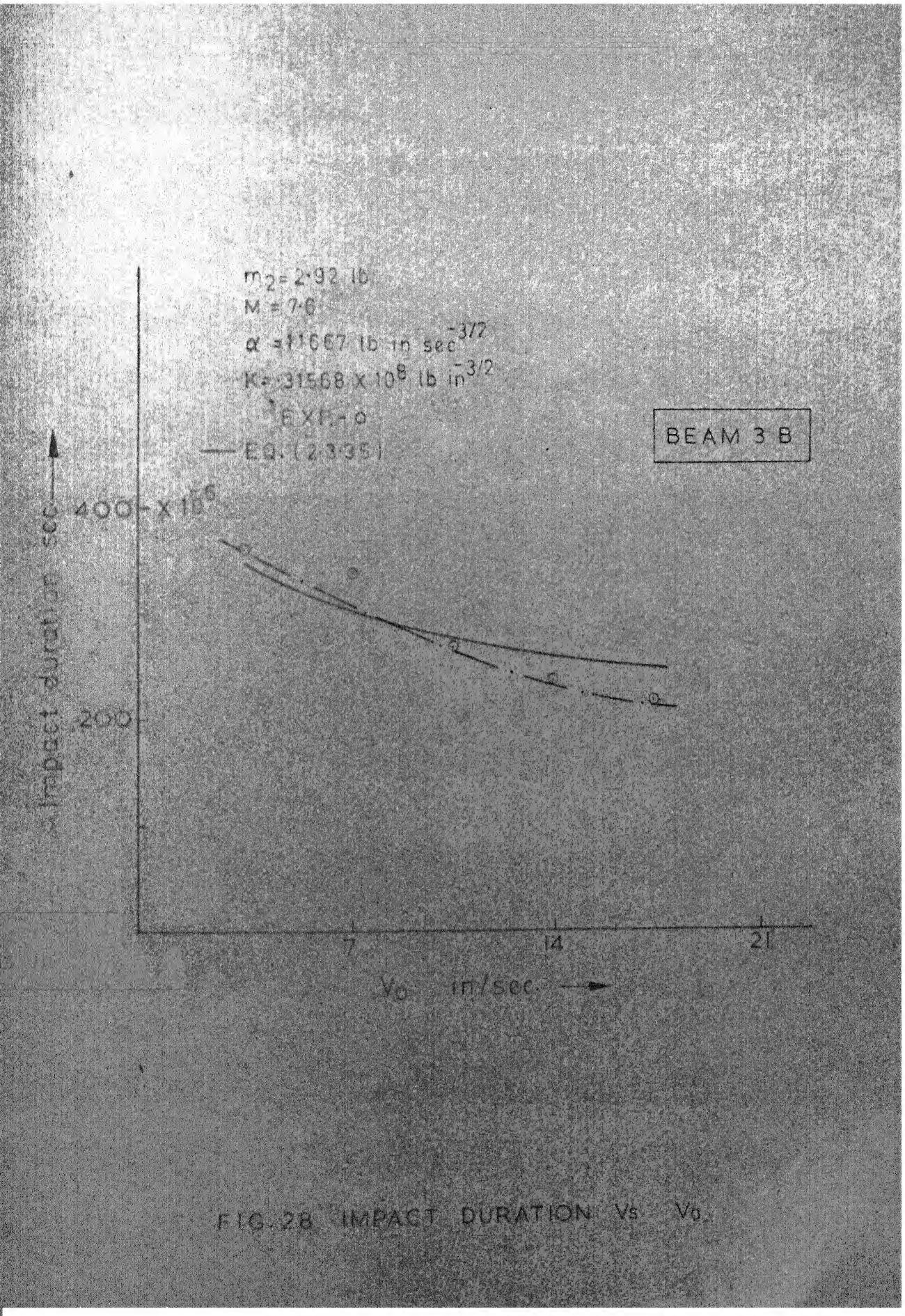

FIG. 28 IMPACT DURATION V_s V_0

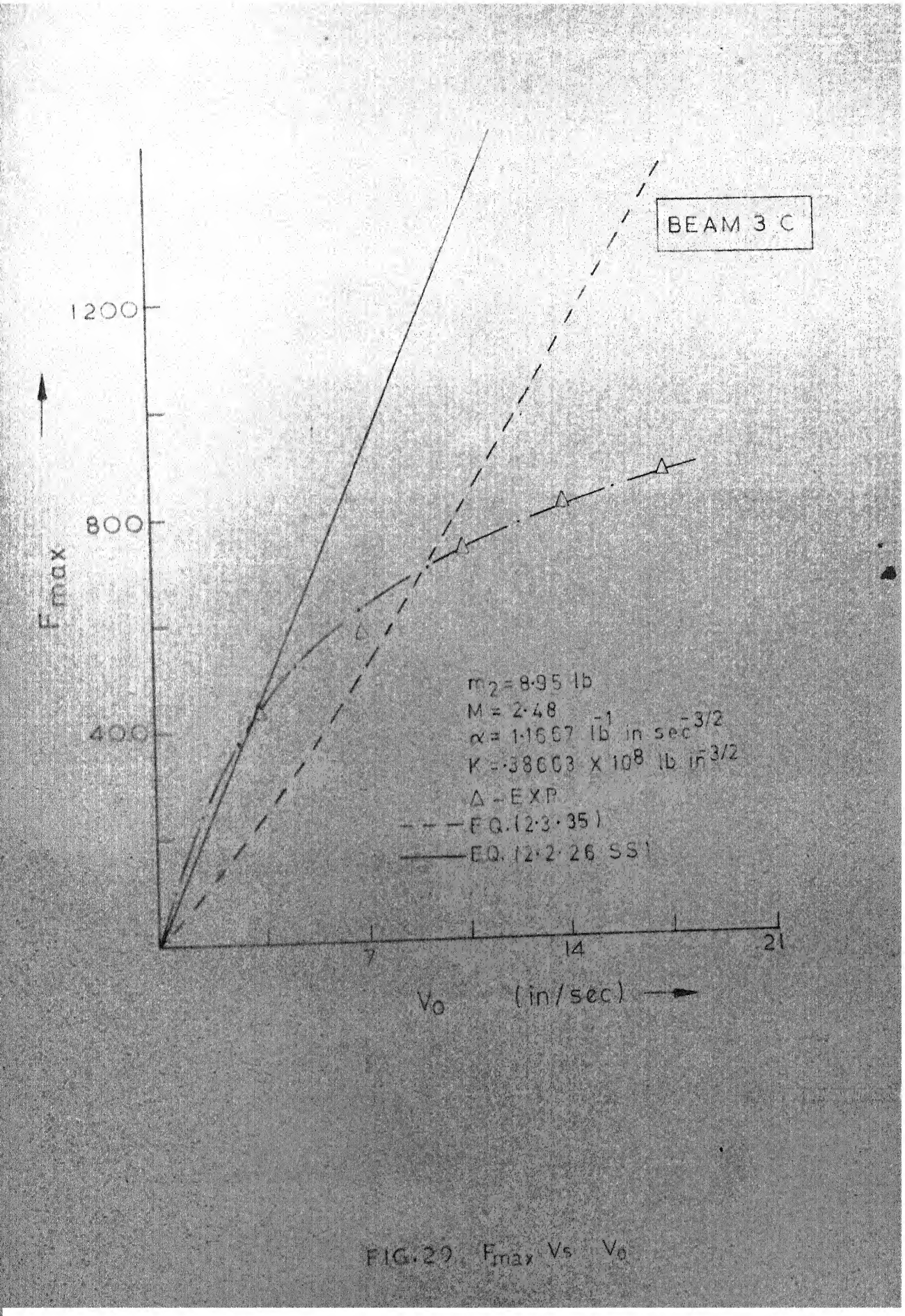

FIG. 29 F_{max} Vs V_0

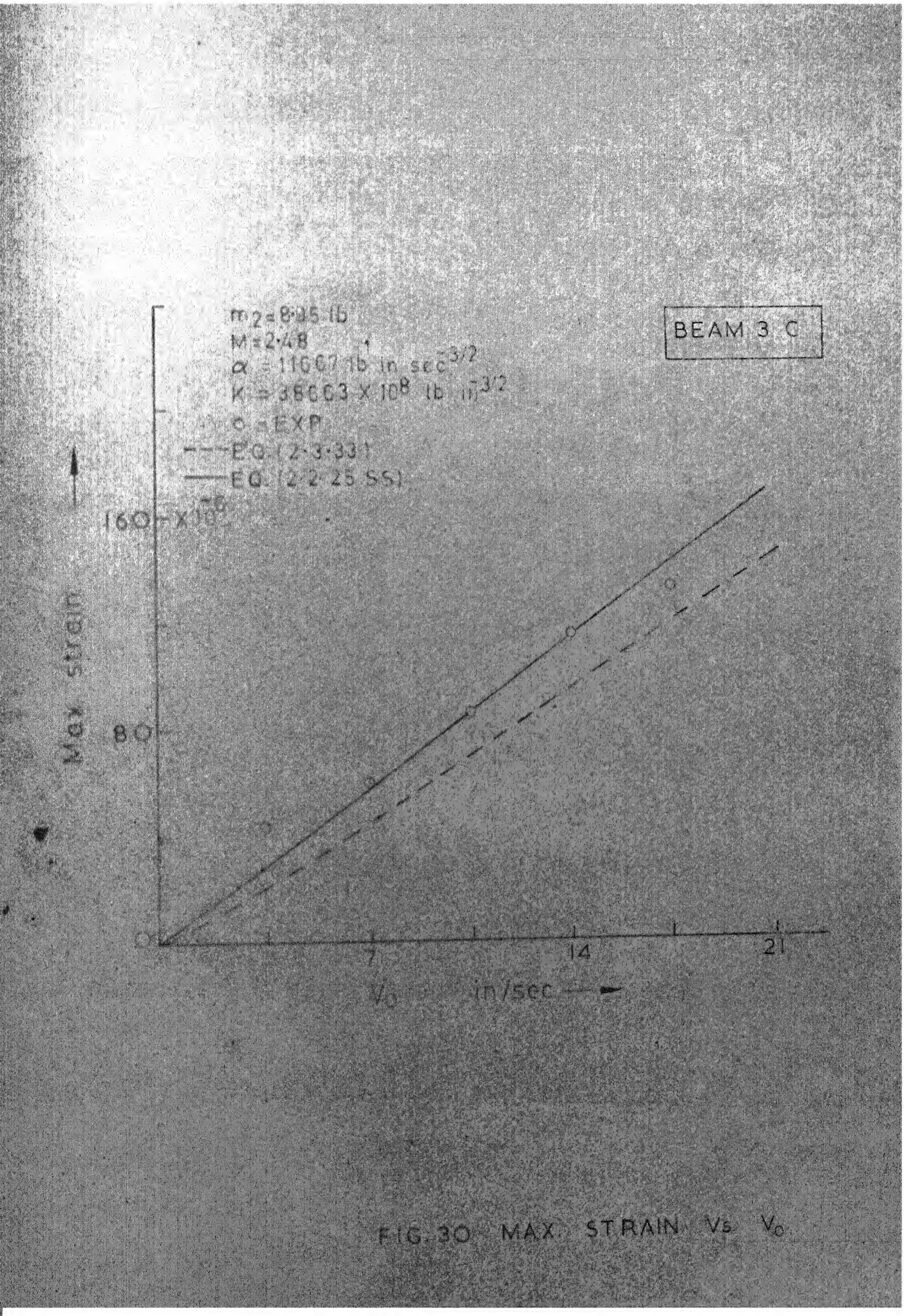

FIG. 30 MAX. STRAIN Vs V_0

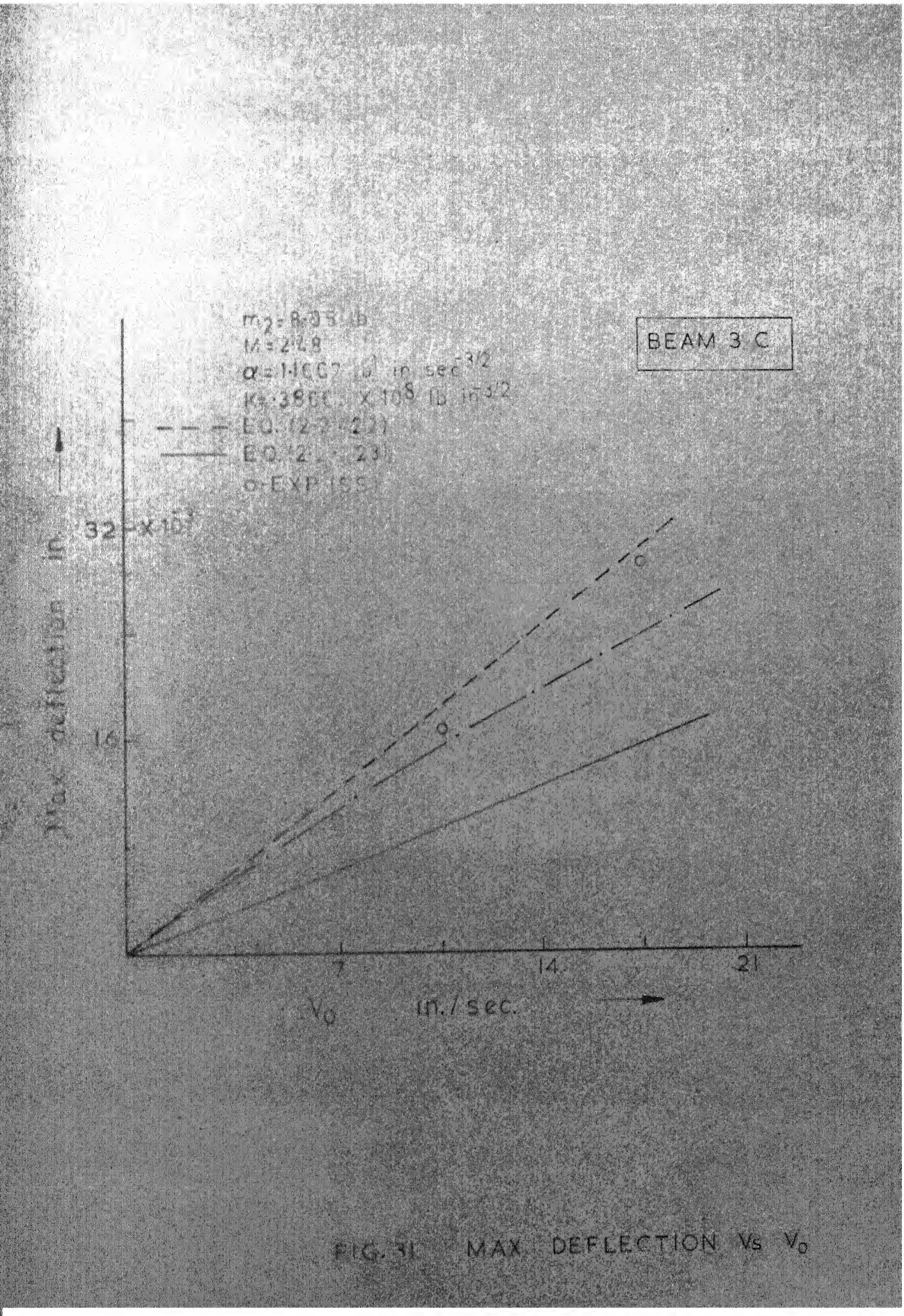

FIG. 31 MAX. DEFLECTION Vs V_0

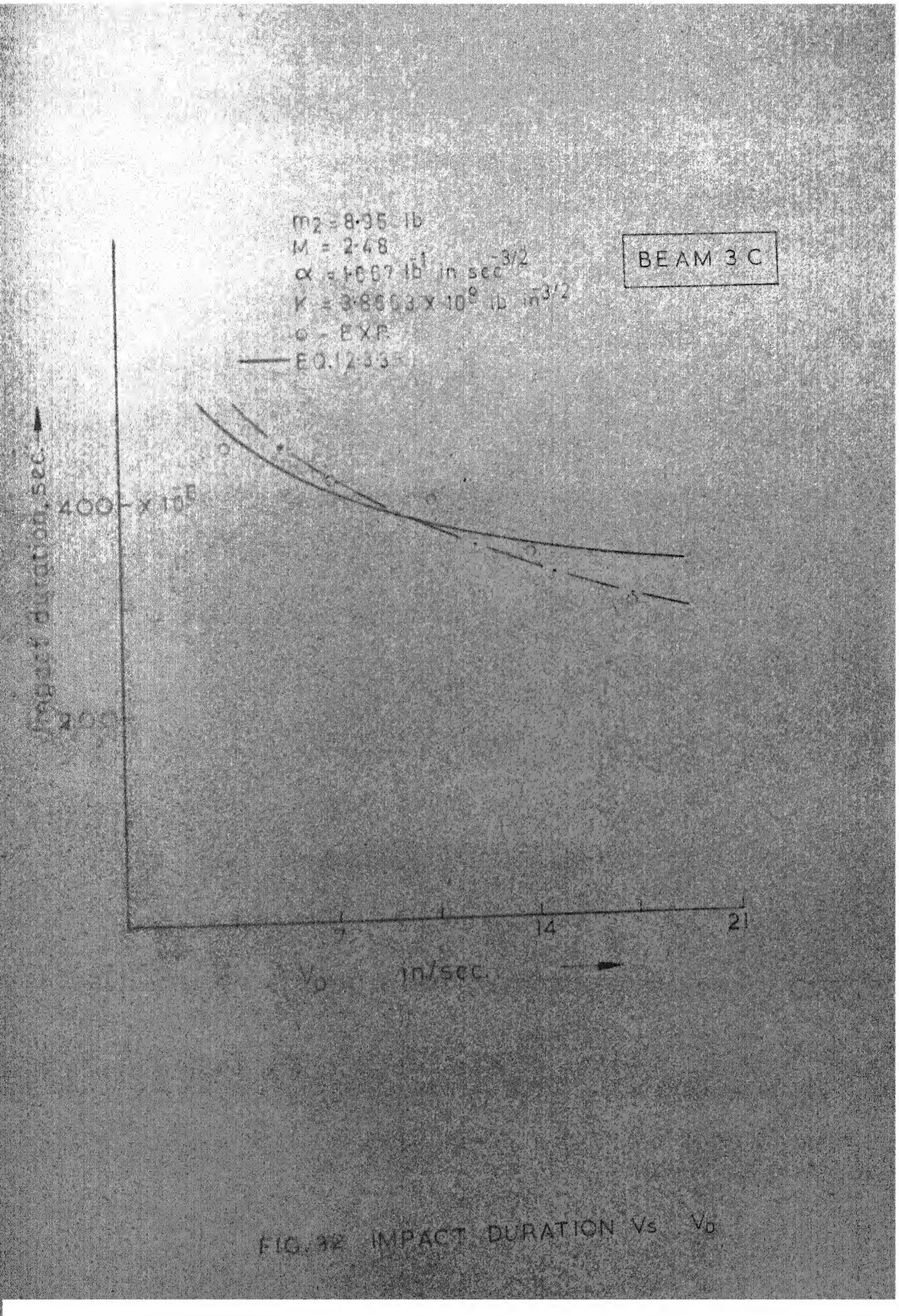

FIG. 32 IMPACT DURATION Vs V_0

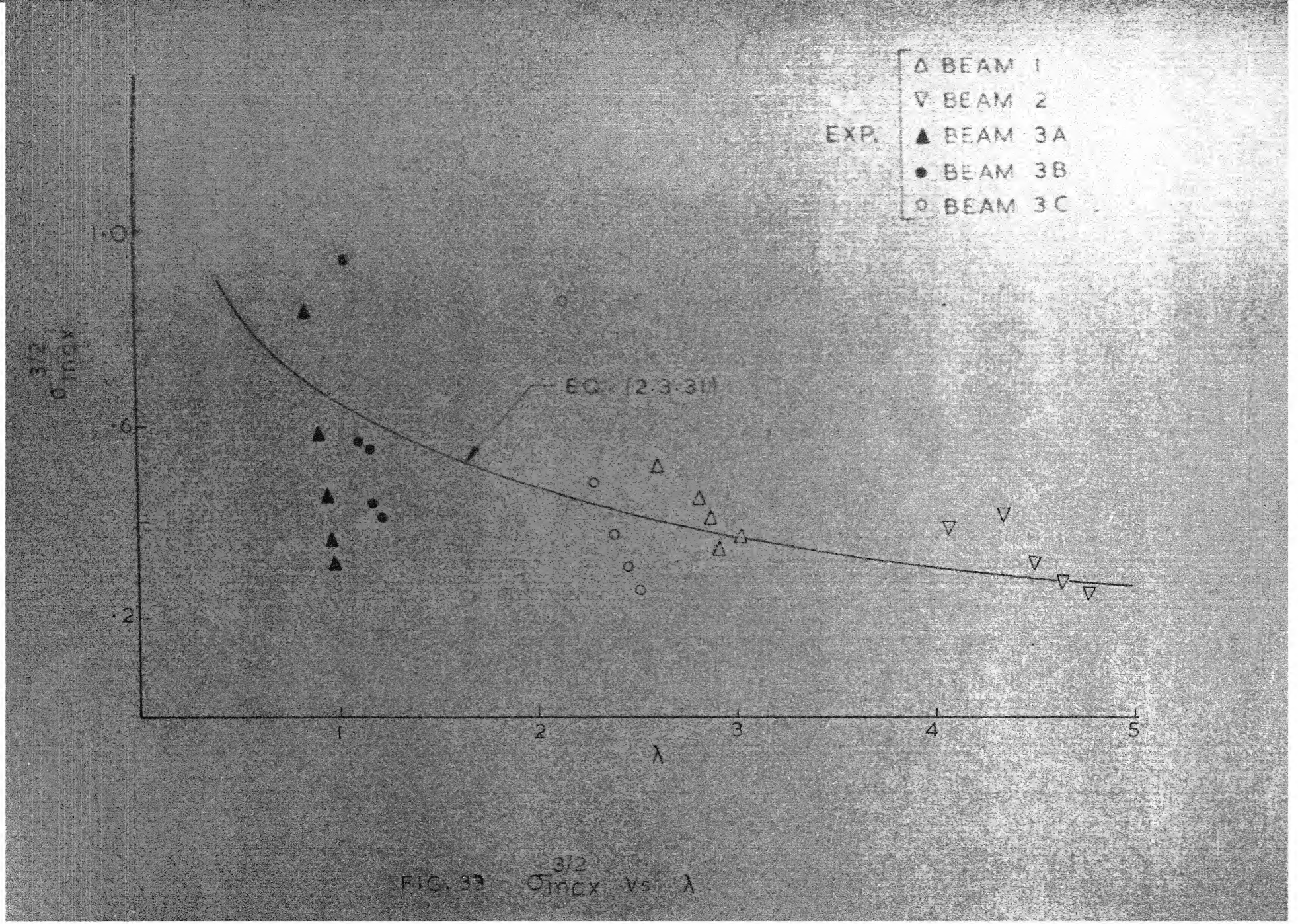

FIG. 39 $\sigma^{3/2}_{max}$ vs. λ

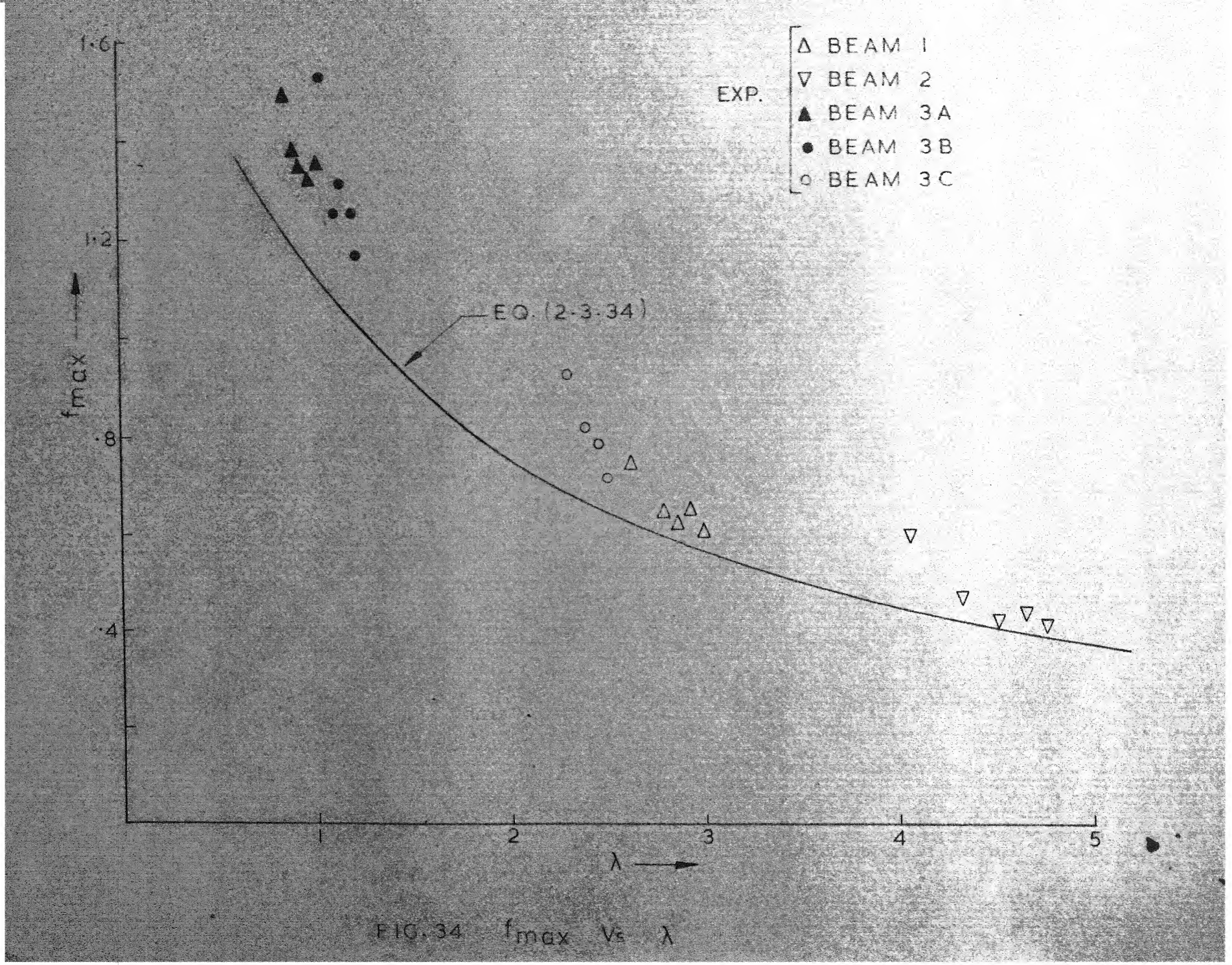

FIG. 34 f_{max} Vs λ

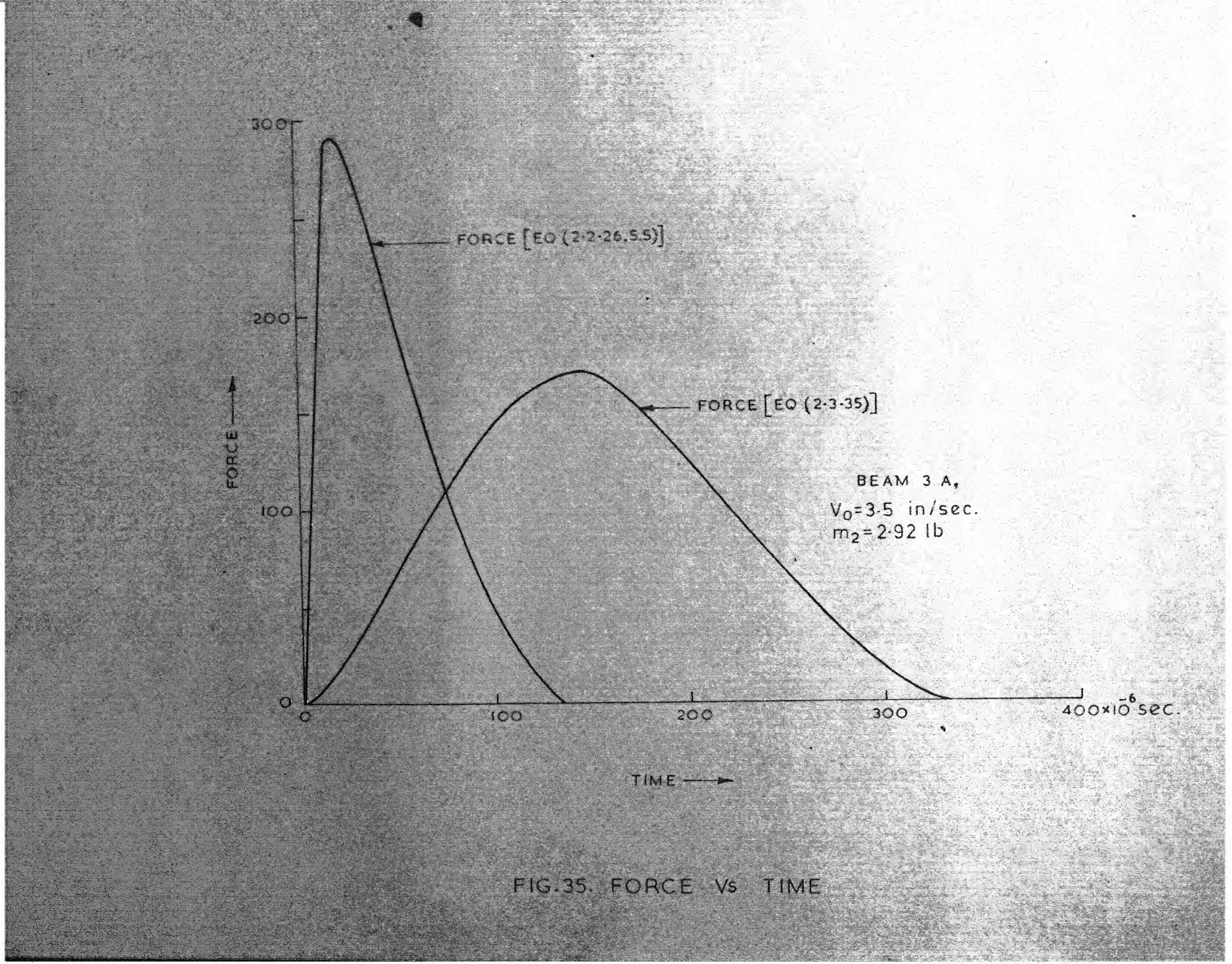

FIG.35. FORCE Vs TIME

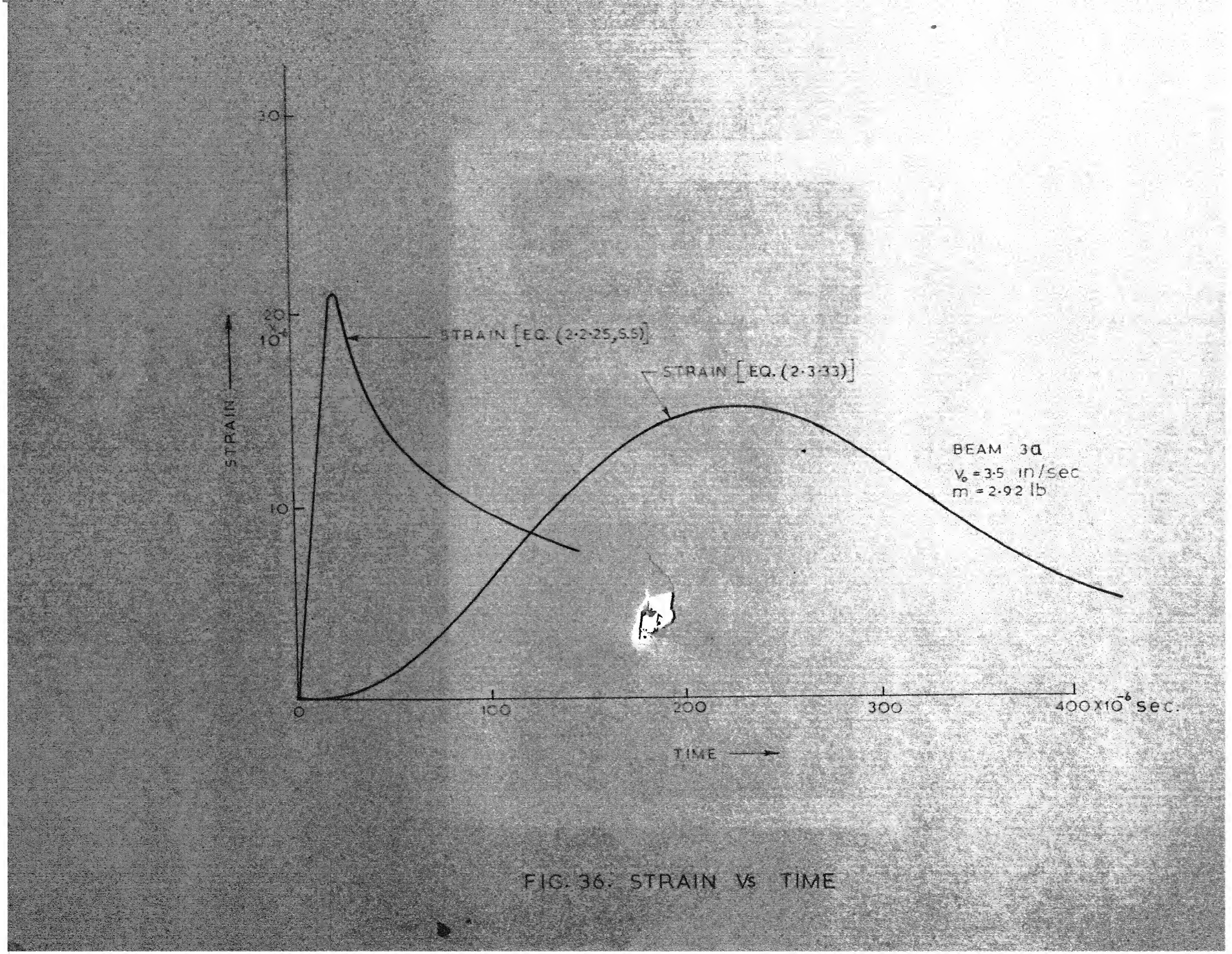

FIG. 36. STRAIN Vs TIME

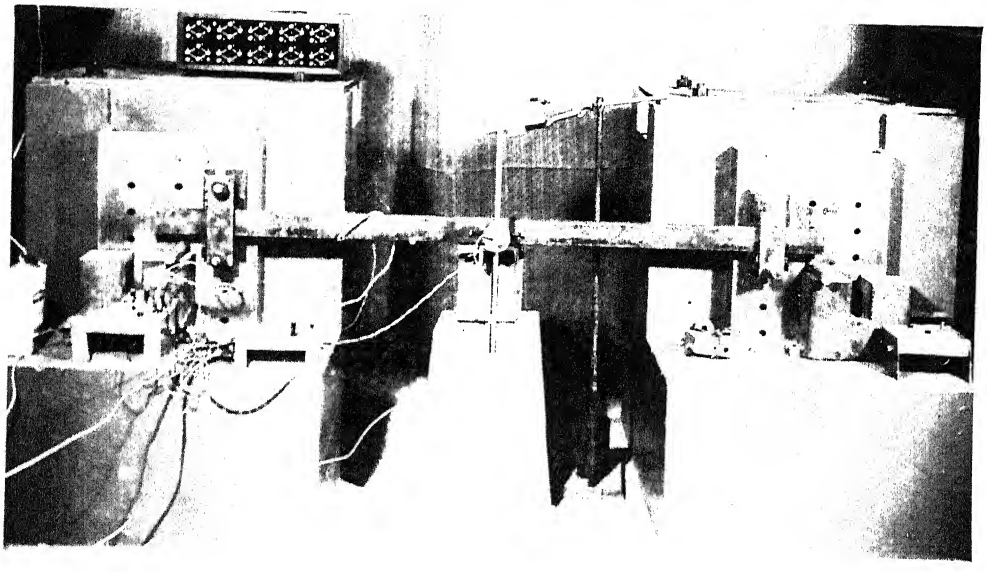

PLATE 1. Lower Part of Set-up

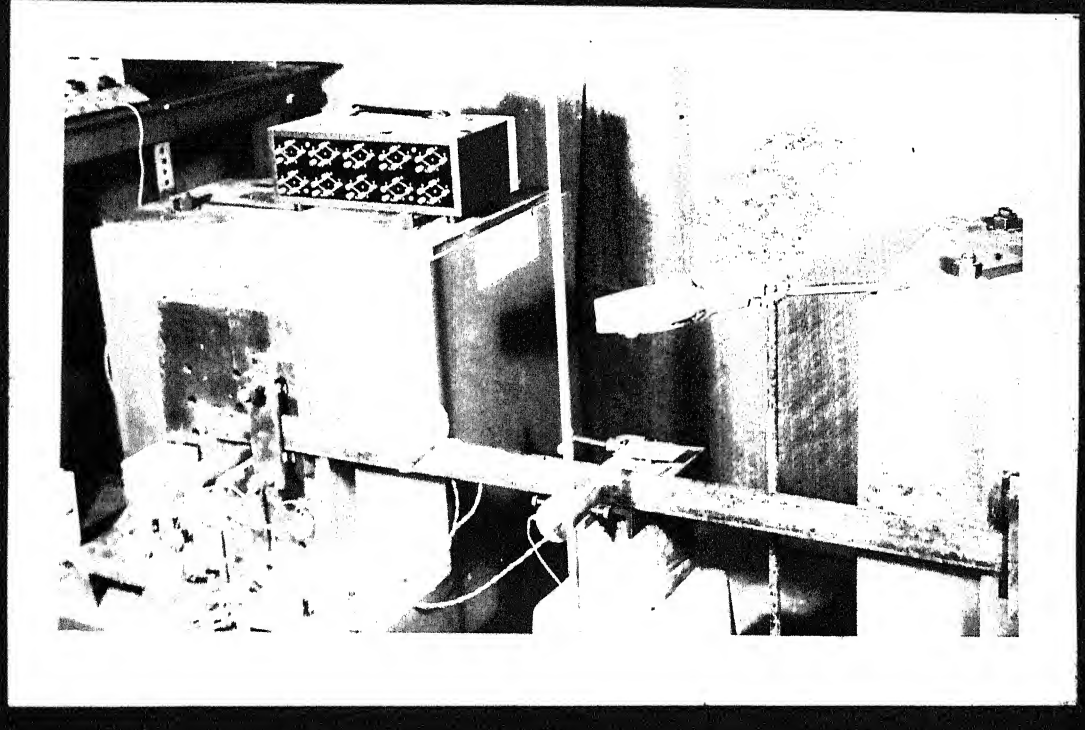

PLATE 2. Supports and Beam in Position

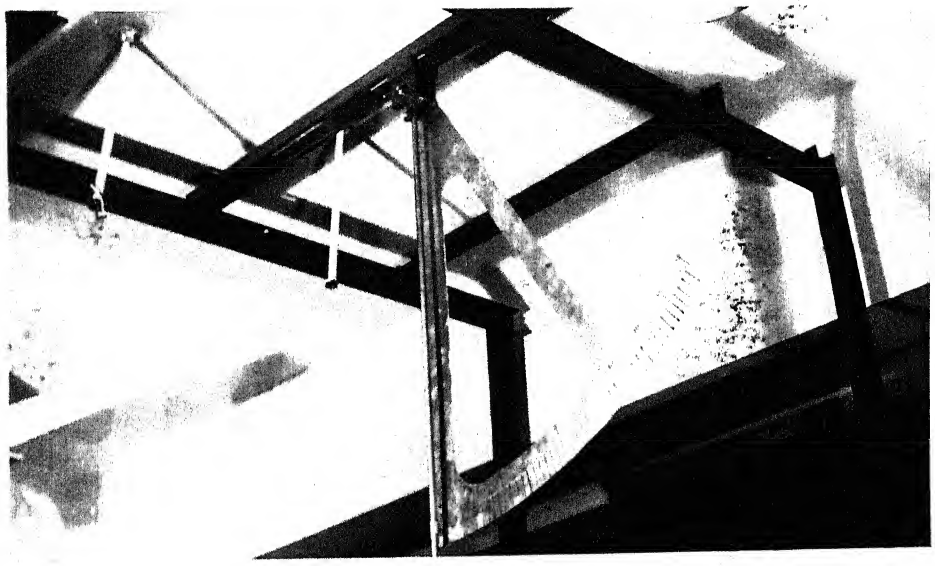

PLATE 3. Top View of Structure

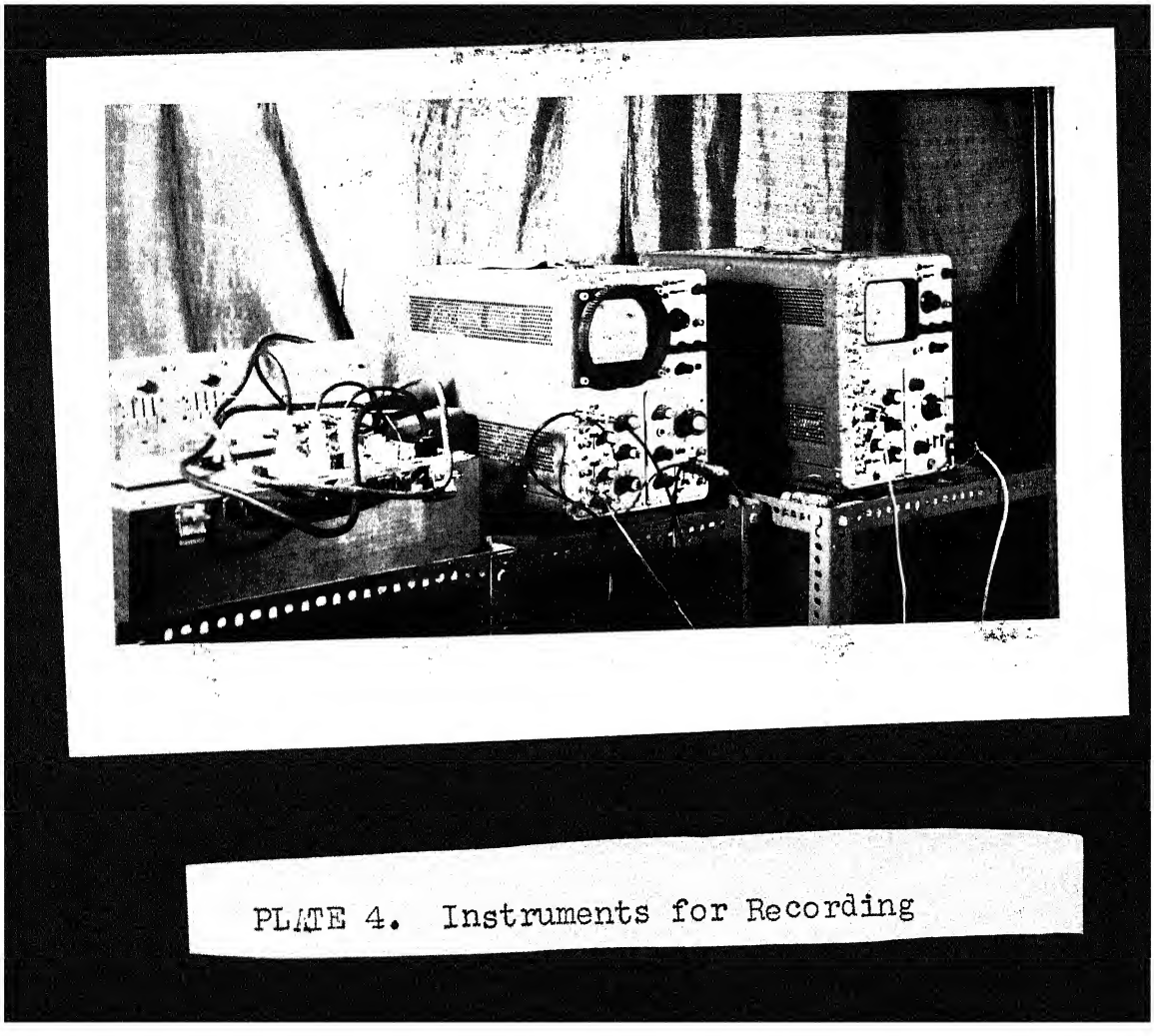

PLATE 4. Instruments for Recording

REFERENCES

1. Thomas Young and J. Johnson, "Natural Philosophy" London 1807, Vol. 1, p 147, vol. 2, p. 50.

2. E. Hodgkinson, "On the Effect of Impact on Beams", Report of the British Association for the Advancement of Science, Third Meeting 1833, pp 421-422.

3. H. Cox, "On Impact on Elastic Beams", Transactions of the Cambridge Philosophical Society, 1856, vol. 9, part 1, p 73.

4. Report of Commissioners Appointed to Inquire into the Application of Iron to Railway Structures - Her Majesty's Stationery Office, London, 1849, pp 39-42.

5. A.J. Saint Venant and A. Flamant, "Theorie de l'elasticite' des corps solides de clebseh", 1883, note finale on par. 61.

6. Hertz, "Uberdic Berührung Fester Elastischer Körper," Journal of Reine Angew Math(crelle) 92, 1881, p 155.

7. S. Timoshenko, "Vibration Problems in Engineering", D. Van Nostrand Co. Inc., New York, N.Y. 1937, p 349.

8. C. Zener, "A Method of Calculating Energy Losses during Impact," Trans. ASME, 1939, A-67.

9. E.H. Lee, "The Impact of Mass Striking a Beam", Trans. ASME, 1949, Vol. 62, A-129.

10. H.L. Mason, "Impact on Beams", Trans. ASME, 1936, Vol. 3, No. 2, A-55.

11. Ludwig Föppl, "Slow Motion Pictures of Impact Test by Means of Photoelasticity", Trans. ASME, 1949, June, p. 173.

12. A.C. Eringen, "Transverse Impact on Beams and Plates," Journal of App. Mech. 1953, p 461.

13. Horst Schweiger, "A Simple Calculation of the Transverse Impact on Beams and its Experimental Verification", Exp. Mechanics, Nov. 1965, p. 373.

14. Horst Schweiger, "Central Deflection of a Transversely Struck Beam", Exp. Mechanics, April 1970, p 166.

15. W. Goldsmith, "Impact", Edward Arnold Pub. Ltd. 1960, p. 64, 82.

16. H. Schmidt, Technische Hochschule Darmstadt, Germany (unpublished paper) has shown that this approximation is satisfactory for values $\pi^2/L^2 \cdot (EI/d\rho h)^{1/2} \cdot (t-t') < 0.1$.

17. Publication of 11 of Math. Res. Centre, "Nonlinear Integral Equations", U.S. Army, The Univ. of Wisconsin, p 225.

18. Dove and Adams, "Experimental Stress Analysis and Measurement", Chap. on Strain Gages.

19. H.G. Bernhart and W. Goldsmith, "Stresses in Beams during Transverse Impact", Journal of App. Mech. 24, 1957, 440.

20. Dally and Riley, "Experimental Stress Analysis", Sec. 15.4, p 409.

APPENDIX

1. SPECIFICATIONS OF TRANSDUCERS

(a) SOLAR CELL

Size 1.1/8" x 1.1/8" x 3/16"

Capacity, Volts .3 to .45 V

Capacity, MA 10-16

Cat. No. S1M

(b) ACCELEROMETER

i) Endevco, Model 2215

Voltage sensitivity with 300 pF external capacitance =14.5 mV/g

Capacitance 10850 pF.

ii) Endevco, Model 2225

Voltage sensitivity with 300 pF external capacitance =.5 mV/g.

(c) STRAIN GAGES

Make - Rohits Co. (India)

Internal Resistance 120.6$\pm$ .1 ohms

Gage factor 2.06 $\pm$ .02

2. FINITE DIFFERENCE METHOD FOR SOLVING EQ.(2.3.31)

Eq.(2.3.31) is a non-linear Volterra integral the general form of which can be given as [17]

$$y(x) = g(x) + \int_{0}^{x} K[x,t \; ; \; y(t)]\, dt \qquad (1)$$

On setting x = 0, h, 2h .....rh in succession in eq.(1) and using the trapezoidal rule for numerical integration the value of y(x) at r^{th} station is given as

$$Y_{r+1} = g_{r+1} + U_{r+1} + \tfrac{1}{2} hK (x_{r+1}, x_{r+1}; Y_{r+1}) \qquad (2)$$

where

$$U_{r+1} = h \left[\tfrac{1}{2} K(x_{r+1}, x_o; Y_o) + \sum_{s=1}^{r} K (x_{r+1}, x_s; Y_s) \right]$$

Eq.(2) is solved iteratively by means of the procedure :

$$Y_{r+1}^{(p+1)} = g_{r+1} + U_{r+1} + \tfrac{1}{2} h\, K(x_{r+1}, x_{r+1}, Y_{r+1}^{(p)}) \qquad (3)$$

where p = 0, 1, 2, ..., and $Y_{r+1}^{(p)}$ is the p^{th} approximation to Y_{r+1}.

The following Predictor-Corrector method with only one iteration process gives good approximation to

the value of Y_{r+1} with an error of the order of (h^2).

Predictor

$$Y^{(o)}_{r+1} = g_{r+1} + U_{r+1} + \tfrac{1}{2} hK (x_{r+1}, x_r; Y_r) \quad (4)$$

Corrector

$$Y_{r+1} = g_{r+1} + U_{r+1} + \tfrac{1}{2} hK (x_{r+1}, x_{r+1}; Y^{o}_{r+1}) \quad (5)$$

where U_{r+1} has been defined in eq. (2).

COMPUTER PROGRAMME-LISTING

```
CC      CHARACTERISTICS ROOTS FOR SIMPLY SUPPORTED CASE
        DIMENSION PHIS(50),PHIC(50)
        AM=2.48
        PYE=4.*ATAN(1.)
        X1S=1.5
        X2S=1.4
        X1=2.
        X2=2.1
        N=40
        DO120 I=1,N
 121    TH1=SINH(X1S)/COSH(X1S)
        TH2=SINH(X2S)/COSH(X2S)
        FO=2.*AM-X1S*(TAN(X1S)-TH1)
        FN=2.*AM-X2S*(TAN(X2S)-TH2)
        XN=FN*X1S/(FN-FO)+FO*X2S/(FO-FN)
        X1S=X2S
        X2S=XN
        IF(ABS(XN-X1S).LT..001)GO TO 122
        GO TO 121
 122    PHIS(I)=XN
        X1S=PHIS(I)+PYE
        X2S=X1S+.1
        PUNCH 888,PHIS(I)
 120     CONTINUE
CC      CHARACTERISTICS ROOTS FOR CLAMPED BEAM
        DO123I=1,N
 124    CZ1=1.-COS(X1)*COSH(X1)
        CZ2=1.-COS(X2)*COSH(X2)
        FO=AM-X1*CZ1/(SIN(X1)*COSH(X1)+COS(X1)*SINH(X1))
        FN=AM-X2*CZ2/(SIN(X2)*COSH(X2)+COS(X2)*SINH(X2))
        XN=FN*X1/(FN-FO)+FO*X2/(FO-FN)
        X1=X2
        X2=XN
        IF(ABS(XN-X1).LT. .001)GO TO 125
        GO TO 124
 125    PHIC(I)=XN
        X1=PHIC(I)+PYE
        X2=X1+0.1
        PUNCH888,PHIC(I)
 123    CONTINUE
 888    FORMAT(1X,E15.5)
        STOP
        END
$ENTRY
```

```
CC      METHOD FOR SOLVING EQS. IN SEC.(2.2)
CC      AM=MASS RATIO =M1/M2
        DIMENSION PHIS(40),PHIC(40),FS(50),FC(50)
        DIMENSION DEFS(50),DEFC(50),STRENS(50),STRENC(50)
        DIMENSION DEGREE(6)
        DATA DEGREE/1.,2.,3.,4.,5.,6./
        AM=2.48
        SM=8.95/(32.2*12.)
        DO120I=1,40
 120    READ 888,PHIS(I)
        DO121I=1,40
 121    READ888,PHIC(I)
 888    FORMAT(1X,E15.5)
        PYE=4.*ATAN(1.)
        AL=40.125
        DO 6IJ=1,6
        DO5I=1,50
        STRENS(I)=0.
        ST-ENC(I)=0.
        DEFS(I)=0.
        FS(I)=0.
        FC(I)=0.
 5      DEFC(I)=0.
        TW=0.
        THETA=PYE*DEGREE(IJ)/180.
        VO=SQRT(2.*32.2*12.*104.25*(1.-COS(THETA)))
        PRINT 11
        PRINT 55,VO
        ROW=.283/(32.2*12.'
        D=1.995
        H=.976
        EI=30.5*10.*M6*D*H**3/12.
        A=(EI/(ROW*DMH))**.25
        PRINT 11
        PRINT 22,A,AM,EI,VO
        PR+NT 11
        PRINT 33
        DO1I=2,50
        II=I-1
        FFS=FS(I-1)*16.*A**2*VO/AL**2*SM
        FFC=FC(I-1)*8.*A**2*VO/AL**2   *SM
        WS=DEFS(I-1)MAL**2'VO/A**2
        WC=DEFC(I-1)MAL**2*VO/(A**2)*1./4.*2.
        SS=STRENS(I-1)*2.*VO*H/A**2
        SC=STRENC(I-1)*VO*H/A**2
        T=TW*AL**2/(4.*A**2)
        PRINT44,II,TW,WS,WC,SS,SC,T,FFS,FFC
        TW=TW+.0005
```

```
      DO2J=1,10
      PHS=PHIS(J)
      PHC=PHIC(J)
      TMT=TAN(PHS)-TANH(PHS)
      TPT=TAN(PHS)+TANH(PHS)
      CCP=1./COS(P+S)**2-1./COSH(PHS)**2+2.*AM/PHS**2
      S1=SIN(TW*PHS**2)
      S2=SIN(TW*PHC**2)
      COCO=COSH(PHC)-COS(PHC)
      SISI=SINH(PHC)+SIN(PHC)
      DEFS(I)=DEFS(I)+TMT*S1/(PHS**3*CCP)
      STRENS(I)=STRENS(I)+TPT*S1/(PHS*CCP)
      FS(I)=FS(I)+TMT*S1*PHS/CCP
      BRK=(1.-COS(PHC)*COSH(PHC))*(COS(PHC)-COSH(PHC))*(SIN(PHC)+SINH(P
     1HC))/((1.-COS(PHC)*COSH(PHC))**2+AM*(COS(PHC)-COSH(PHC))**2)
      DEFC(I)=DEFC(I)+BRK*S2*((SINH(PHC)-SIN(PHC))/COCO-(COSH(PHC)
     1-COS(PHC))/SISI)/PHC**2
      STRENC(I)=STRENC(I)+BRK*((SINH(PHC)+SIN(PHC))/COCO-(COSH(PHC)+
     1COS(PHC))/SISI)*S2
      FC(I)=FC(I)+BRK*S2*PHC**2*((SINH(PHC)-SIN(PHC))/COCO-(COSH(PHC)-
     1COS(PHC))/SISI)
   2  CONTINUE
C  ---------------CONTROL FOR OVERFLOW
      DO14K=11,25
      PHS=PHIS(K)
      PHC=PHIC(K)
      S1=SIN(TW*PHS**2)
      S2=SIN(TW*PHC**2)
      DEFS(I)=DEFS(I)+TAN(PHS)*S1/(1./(COS(PHS))**2+2.*AM/PHS**2)/PHS**3
      COCO=COSH(PHC)-COS(PHC)
      SISI=SINH(PHC)+SIN(PHC)
      STRENS(I)=STRENS(I)+TAN(PHS)*S1/(1./(COS(PHS))**2+2.*AM/PHS**2)/PH
     1S
      FS(I)=FS(I)+TAN(PHS)*S1*PHS/(1./(COS(PHS))**2+2.*AM/PHS**2)
      BRK=SINH(PHC)*COS(PHC)/(COS(PHC)**2+AM)
      DEFC(I)=DEFC(I)+BRK*S2*((SINH(PHC)-SIN(PHC))/COCO-(COSH(PHC)-COS
     1(PHC))/SISI)/PHC**2
      STRENC(I)=STRENC(I)+BRK*((SINH(PHC)+SIN(PHC))/COCO-(COSH(PHC)+
     1COS(PHC))/SISI)*S2
      FC(I)=FC(I)+BRK*S2*PHC**2*((SINH(PHC)-SIN(PHC))/COCO-(COSH(PHC)-
     1COS(PHC))/SISI)
  14  CONTINUE
   1  CONTINUE
   6  CONTINUE
  11  FORMAT(/1X,120(1H-))
  22  FORMAT(1X,*A=*,E16.5,3X,*AM=*,E16.5,3X,*EI=*,E16.5,3X,*VO=*,E16.5
     1)
  33  FORMAT(2X,*I NO*,8X,*TW*,14X,*WS*,14X,*WC*,14X,*SS*,14X,*SC*,14X,
     1*T*)
  44  FORMAT(2X,I4,8E15.5)
  55  FORMAT(1X,*VO=*,E16.5)
      STOP
      END
$ENTRY
```

54

FINITE DIFFERENCE TECHNIQUE

```
CC      EZK=HERTZ CONSTANT ,T=REF. TIME
CC      ALMD=IMPACT PARAMETER ,ALFA=BEAM PARAMETER
$EXECUTE        WATFOR,REWIND
$IBFTC MAIN
        DIMENSION SIGMA(51),TOW(51),FTL(51),DEF(51)
        DIMENSION PT(51),W(51)
        DIMENSION V0(6)
        DIMENSION DEGREE(6)
        DATA DEGREE/1.,2.,3.,4.,5.,6./
        R=104.125
        R1=3.
        E=30.5*10.**6
        EZK=.666*E*SQRT(R1)/.91
        D=1.995
        H=.976
        ROW=.283/(32.2*12.)
        SM=8.95
        SM=SM/(32.2*12.)
        PYE=4.*ATAN(1.)
        EI=D*H**3*E/12.
        DO3I=1,6
        THETA=PYE*DEGREE(I)/180.
    3   V0(I)=SQRT(2.*32.2*12.*R*(1.-COS(THETA)))
        DO 19IJ=1,6
C-----T-REFERENCE TIME
C-----ALMD-IMPACT PARAMETER
C-----TOW-T/REF.TIME
C-----SIGMA---(W-W0)/T*V0
C-----ALFA--BEAM PARAMETER
        T=(SM**.4)/(EZK**.4*V0(IJ)**.2)
        PRINT55,T,EZK
        ALFA=(D*ROW*H/EI)**.25/(SQRT(2.*PYE)*D*ROW*H)
        ALMD=(ALFA*SM)/SQRT(T)
        PRINT44,ALMD,ALFA,V0(IJ)
        TOW(1)=0.
        DO 100I=1,50
 100    TOW(I+1)=TOW(I)+.1
        SIGMA(1)=0.
        AH=.1
C-----TIME INTERVAL FOR TOW
        DO 10I=2,51
        II=I-1
C-----PREDICTOR
        SUM=0.
        DO 9J=1,II
   9    SUM=SUM+(SIGMA(J)**1.5)*(TOW(I)-TOW(J)+ALMD*(TOW(I)-TOW(J))**.5)
        CALC=AH*(.5*SIGMA(1)**1.5*(TOW(I)-TOW(1)+ALMD*(TOW(I)-TOW(1))**.5
       1)+SUM)
        SIGMA(I)=TOW(I)-CALC-.5*AH*SIGMA(II)**1.5*(TOW(I)-TOW(II)+ALMD*
       1(TOW(I)-TOW(II))**.5)
        IF(SIGMA(I).GE.0.)GO TO 10
```

```
      IF(SIGMA(I).LT.0.)N=I-1
      GO TO 7
C     BUT HERE IT IS NOT NEEDED
 10   CONTINUE
C--0--CORRECTOR
C-----STRAIN  AS FN. OF TIME
    7 FTL(1)=0.
      DEF(1)=0.
      DO8I=2,N
      IF((SIGMA(I)-SIGMA(I-1)).GE.0.)MAX=I
      II=I-1
      SUM=0.
      SUMD=0.
      DO2OJ=1,II
      SUMD=SUMD+SIGMA(J)**1.5*(TOW(I)-TOW(J))**.5
 20   SUM=SUM+SIGMA(J)**1.5*(TOW(I)-TOW(J))**(-.5)
      FTL(I)=AH*(.5*SIGMA(1)**1.5*(TOW(I)-TOW(1))**.5+SUM)
      DEF(I)=AH*(.5*SIGMA(1)**1.5*(TOW(I)-TOW(1))**.5+SUMD)
 8    CONTINUE
      PRINT11
      DO 30I=1,N
      SIMA=SIGMA(I)**1.5
 30   PRINT22,I,SIMA,FTL(I),TOW(I)
      SIMAX=SIGMA(MAX)**1.5
      PRINT33,MAX,SIMAX,FTL(MAX)
C
C     CALCULATION OF FORCE ,STRAIN, DISPLACEMENT
C
      PRINT 77
      DO 40 I=1,N
      SIMA=SIGMA(I)**1.5
      PT(I)=EZK*SIMA*(T*V0(IJ))**1.5
      ST1=1.732*(ROW/E)**.5*(ALFA/2.)*EZK*V0(IJ)**1.5*T**2*FTL(I)
      TIME=TOW(I)*T
      W(I)=EZK*ALFA*V0(IJ)**1.5*T**3*DEF(I)
      PRINT 66,I,PT(I),ST1,W(I),TIME
 40   CONTINUE
 66   FORMAT(1X,I6,4E16.5)
 77   FORMAT(/1X,*STEP   *,5X,*FORCE *,10X,*STRAIN *,5X,*DEFLECTION */)
 19   CONTINUE
 11   FORMAT(5X,*STEP*,12X,*(SIGMA)1.5*,5X,*FTL(I)*,10X,*REF TIME*)
 22   FORMAT(5X,I6,10X,3E16.5)
 33   FORMAT(1X,120(1H-),/,1X,*MAX=*,I5,*SIMAX=*,E16.5,10X,*FTL(MAX)=*,
     1E16.5,/,120(1H-))
 44   FORMAT(1X,120(1H-),/,1X,*ALMD=*,E16.5,10X,*ALFA=*,E16.5,*V0=*,E16
     1.5,/,1X,120(1H-))
 55   FORMAT(//,50X,*T=*,E16.5,*EZK=*,E16.5)
      STOP
      END
$ENTRY
```
